ACS OMEGA

http://pubs.acs.org/journal/acsodf

Article

Synthesis of B/Si Bidentate Lewis Acids, *o*-(Fluorosilyl)borylbenzenes and *o*-(Difluorosilyl)borylbenzenes, and Their Fluoride Ion Affinities

Junpei Shimada, Atsushi Tani, Chihiro Hanazato, Takashi Masuyama, Yohsuke Yamamoto, and Atsushi Kawachi*

Cite This: *ACS Omega* 2022, 7, 30939−30953

Read Online

ACCESS | Metrics & More | Article Recommendations | Supporting Information

ABSTRACT: Herein, we report detailed studies on a series of *o*-(silyl)(boryl)benzenes (**1**−**4**), in which the two Lewis acid centers consisting of silicon and boron atoms are linked via an *o*-phenylene skeleton. *o*-(Fluorosilyl)(dimesitylboryl)benzenes **1** and **2** were prepared by the reaction of fluorodimesitylborane with [*o*-(fluorodimethylsilyl)phenyl]lithium (**7**) and [*o*-(fluorodiphenylsilyl)phenyl]lithium (**8**), respectively. *o*-(Difluorosilyl)(dimesitylboryl)benzenes **3** and **4** were also prepared by the reaction of fluorodimesitylborane with *o*-{[di(methoxy)methylsilyl]phenyl}lithium (**11**) and *o*-{[di(methoxy)phenylsilyl]-phenyl}lithium (**12**), respectively, and their subsequent treatment with HF·pyridine. Compounds **1**−**4** readily capture a fluoride ion in the presence of 18-crown-6 or [2.2.2]cryptand to afford their corresponding μ-fluoro-bridged ate complexes (**15**−**18**). The structures of **15**−**18** were revealed by NMR spectroscopy and X-ray crystallography. DFT studies and natural bond orbital analysis of **15**−**18** were conducted to elucidate the nature of the Si−F and B−F bonding interactions in the μ-fluoro-bridges. The fluoride ion affinities of **1**−**4** were investigated by ^{1}H NMR spectroscopy to monitor their competitive reactions. The dynamic behaviors of **15**−**18** at variable temperatures were monitored using ^{19}F NMR spectroscopy.

B/Si Bidentate Lewis Acids Lined Up!

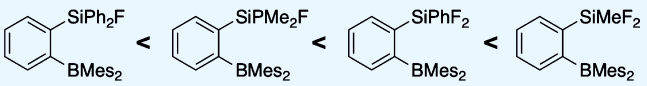

Order of Lewis Acidity

INTRODUCTION

Bidentate Lewis acids bearing two Lewis acid centers have received a great deal of attention in the fields of organic synthesis, molecular recognition, and main group chemistry because they efficiently accept Lewis bases via a reversed chelation mode.[1]

Since the Lewis acidity of tricoordinate boron[2] and tetracoordinate silicon[3] atoms are well recognized, the introduction of these elements into an organic framework is a promising route to construct high-performance bidentate Lewis acids. Thus, homonuclear B/B bidentate Lewis acids **I**−**V**[4] and Si/Si bidentate Lewis acids **VI**−**VIII**[5] have been extensively investigated, as shown in Chart 1.

Heteronuclear B/Si bidentate Lewis acids **IX**−**XI** consisting of silicon and boron centers have attracted an increasing amount of research interest.[6] Katz et al. have applied a 1,8-naphthalene skeleton to construct a B/Si bidentate Lewis acid but found that the skeleton was not suitable for capturing a fluoride ion due to steric congestion.[6a] Aldridge et al. applied a ferrocene skeleton to construct a B/Si bidentate Lewis acid.[6c] Some groups applied several aromatic frameworks to construct a variety of bidentate Lewis acids bearing B/heteroatom centers for fluoride ion recognition.[7,8]

In our previous work, we constructed two B/Si bidentate Lewis acids, *o*-(fluorosilyl)(dimesitylboryl)benzenes **1** and **2**, using a *o*-phenylene skeleton (Chart 2).[9,10] In this context, we have extended this chemistry to the difluorosilyl system, *o*-(difluorosilyl)(dimesitylboryl)benzenes **3** and **4**. Herein, we report the preparation, structure, Lewis acidity, and dynamic behavior of monofluorosilyl and difluorosilyl systems **1**−**4**. The chemistry of mixed Si/B Lewis acids is disclosed in detail and systematically more than ever before.

RESULTS AND DISCUSSION

Preparation of *o*-$C_6H_4(SiR_2F)BMes_2$ 1 (R = Me) and 2 (R = Ph). Li−Br exchange of *o*-(fluorosilyl)bromobenzenes **5** and **6** using *tert*-BuLi in Et_2O at −78 °C affords aryllithium **7** and **8**, which were subsequently reacted with Mes_2BF to yield **1** and **2**, respectively (Scheme 1).[9,10] **1** and **2** were obtained as colorless crystals via recrystallization from hexane.

Preparation of *o*-$C_6H_4(SiRF_2)(BMes_2)$ 3 (R = Me) and 4 (R = Ph). Treatment of [di(methoxy)silyl]bromobenzenes **9** and **10** with *tert*-BuLi at −78 °C gave aryllithium **11** and **12**, which were allowed to react with Mes_2BF at −60 °C for 24 h to form [di(methoxy)silyl]borylbenzenes **13** and **14**, respectively (Scheme 2).[11] Reacting **13** and **14** with an excess

Received: May 6, 2022
Accepted: August 10, 2022
Published: August 23, 2022

Chart 1. Previous Examples of B/B, Si/Si, and B/Si Bidentate Lewis Acids

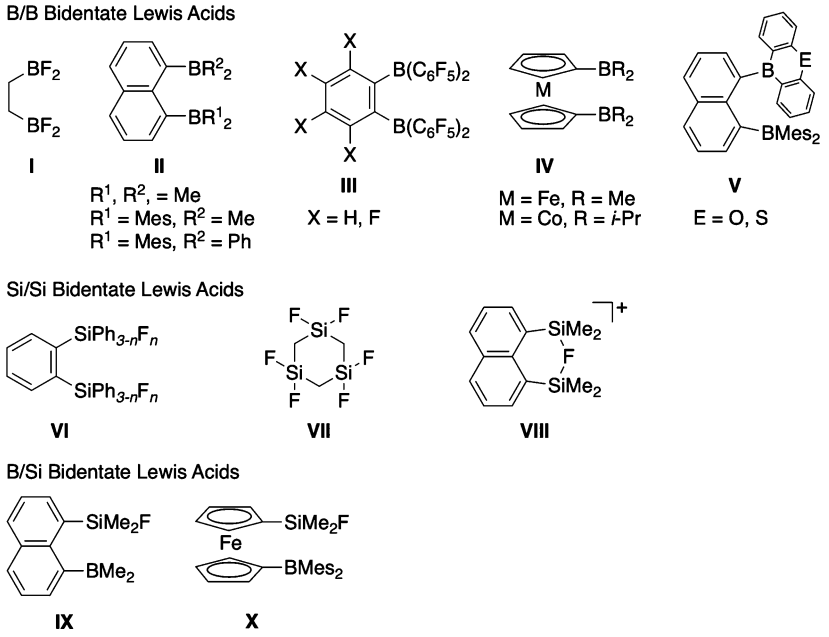

Chart 2. B/Si Bidentate Lewis Acids Described in This Study

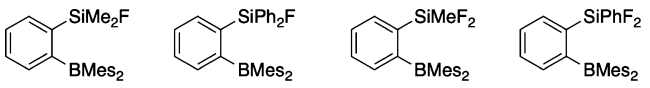

Scheme 1. Preparation of B/Si Bidentate Lewis Acids 1 and 2

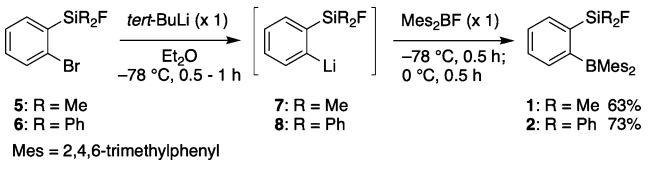

Scheme 2. Preparation of B/Si Bidentate Lewis Acids 3 and 4

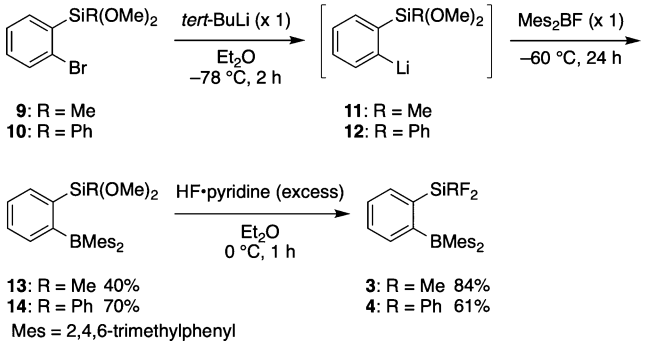

amount of HF·pyridine in Et_2O at 0 °C produces (difluorosilyl)borylbenzenes **3** and **4**, respectively.[12] **3** and **4** were obtained as colorless crystals via recrystallization from hexane.

Formation of μ-Fluoro-bridged Si/B Ate Complexes. *Reaction of **1** and **2** with KF to Form [o-$C_6H_4(SiR_2F)(BMes_2)$-(μ-F)$^-$][K^+L] **15** (R = Me) and **16** (R = Ph).* (Fluorosilyl)-borylbenzenes **1** and **2** capture a fluoride ion from KF in the presence of [2.2.2]cryptand (**a**) or 18-crown-6 (**b**) (= *L*) in toluene at room temperature (Scheme 3).[9] The resulting μ-fluoro-bridged ate complexes (**15** and **16**) were isolated as colorless crystals via recrystallization from THF−hexane.

Scheme 3. Reaction of 1 and 2 with KF to Form 15 and 16

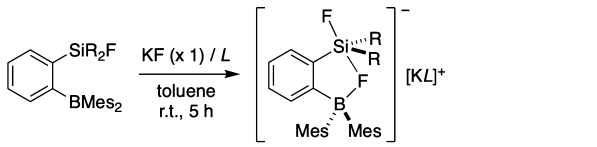

*Reaction of 3 and 4 with KF to Form [o-$C_6H_4(SiR_2F)$-($BMes_2$)(μ-F)$^-$][K^+L] **17** (R = Me) and **18** (R = Ph).* (Difluorosilyl)borylbenzenes **3** and **4** also captured a fluoride ion under the same reaction conditions used for **1** and **2** (Scheme 4). The resulting μ-fluoro-bridged ate complexes (**17** and **18**) were isolated as colorless crystals via recrystallization from hexane.

Solid-State Structures. *Fluorosilyl Derivatives **15** and **16**.* The binding mode for the fluoride ion in μ-fluoro-bridged ate complexes **15** and **16** was revealed using X-ray

Scheme 4. Reaction of 3 and 4 with KF to Form 17 and 18

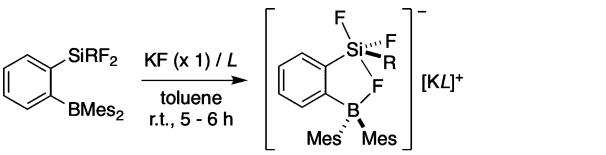

https://doi.org/10.1021/acsomega.2c02775
ACS Omega 2022, 7, 30939−30953

Table 1. Summary of the Crystallographic and Spectroscopic Data Obtained for 15 and 16

$-SiR_{3-n}F_n$	$-SiMe_2F$ (**15a**)	$-SiMe_2F$ (**15b**)	$-SiPh_2F$ (**16a**)	$-SiPh_2F$ (**16b**)
Si−F1 [Å]	1.6440(13)	1.654(2)	1.6516(15)	1.6548(15)
Si···F2 [Å]	2.5309(13)	2.4385(23)	2.2655(14)	2.2481(13)
B−F2 [Å]	1.491(2)	1.492(4)	1.508(2)	1.514(3)
α/β [deg]	124/120	124/119	123/118	122/118
$\Sigma(C-Si-C)_3$ [deg]	349	352	354	354
% TBPe[5b]	65.1	74.6	81.0	81.0
$\delta(^{11}B)$ [ppm]	6 (br)	6 (br)	7 (br)	7 (br)
$\delta(^{19}F)$ [ppm]	−151.9 (br, 1F), −146.8 (d of sept, 1F, $^2J_{F-F}$ = 9 Hz, $^3J_{F-H}$ = 9 Hz)	−151.7 (br, 1F), −146.6 (d of sept, 1F, $^2J_{F-F}$ = 9 Hz, $^3J_{F-H}$ = 9 Hz)	−148.1 (br, 1F), −144.9 (d, 1F, $^2J_{F-F}$ = 18 Hz)	−148.0 (br, 1F), −144.9 (d, 1F, $^2J_{F-F}$ = 18 Hz)
$\delta(^{29}Si)$ [ppm]	6.5 (dd)	6.4 (d)	−32.6 (dd)	−32.7 (dd)
$\Delta\delta(^{29}Si)$ [ppm]	−14.3	−15.0	−29.2	−29.2
$^1J_{Si-F1}$ [Hz]	260	260	266	262
$^1J_{Si-F2}$ [Hz]	7	not observed	17	17

crystallography.[13] The bond lengths and bond angles in **15** and **16** and their NMR data are summarized in Table 1, and their molecular structures are shown in Figures 1 and 2, respectively.

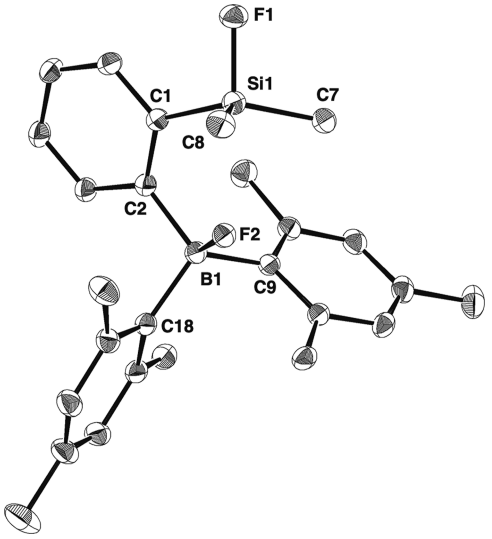

Figure 1. Crystal structure of the anionic part of **15a** (30% thermal ellipsoids).

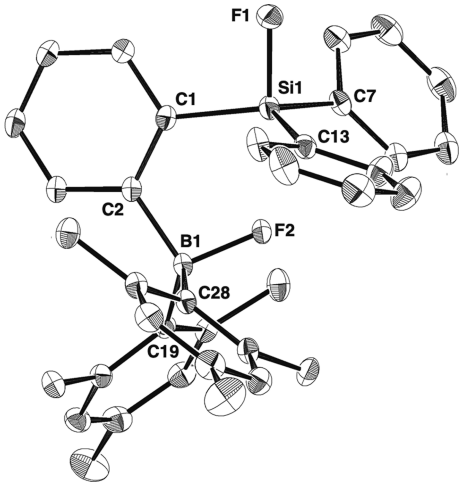

Figure 2. Crystal structure of the anionic part of **16a** (30% thermal ellipsoids).

15a, **16a**, and **16b** exist as separated ion pairs, in which the potassium cation (K^+) is fully coordinated to the cryptand (**15a** and **16a**) or crown ether and a THF molecule (**16b**).[14] On the other hand, **15b** forms a contact ion pair including an interaction between the terminal fluorine (F1) and the potassium cation with a bond distance of 2.81 Å. The bridging fluorine (F2) is tightly bonded to the boron atom (B−F2 = 1.49−1.51 Å) and is also weakly coordinated to the silicon atom (Si−F2 = 2.25−2.53 Å). The two fluorine atoms (F1 and F2) occupy apical positions with a linear alignment (F2−Si−F1 = 175−176°) in a pseudo trigonal bipyramidal (TBP) structure centered at the silicon atom.

*Difluorosilyl Derivatives **17** and **18**.* The structures of difluorosilyl derivatives **17** and **18** (L = [2.2.2]cryptand (**a**) and 18-crown-6 (**b**)) were also revealed using X-ray crystallography.[13] The bond lengths and the bond angles of **17** and **18** are summarized in Table 2, and the molecular structures are shown in Figures 3 and 4, respectively.

Compounds **17a**, **17b**, and **18a** exist as solvent-separated ion pairs. The potassium cation is coordinated to the cryptand (**17a** and **18a**) or crown ether and a THF molecule (**17b**).[14] On the other hand, **18b** is a contact ion pair, in which the two fluorine atoms (F1 and F2) on the silicon atom are coordinated to the potassium cation (F1/F2−K^+ = 2.801(4)/2.712(4) Å). Furthermore, the potassium cation interacts with the C−H moiety of the *o*-phenylene of an adjacent molecule, forming an infinite chain in the solid state. The bridging fluorine (F3) is tightly bound to the boron atom (B−F3 = ca. 1.51−1.57 Å) and weakly coordinated to the silicon atom (Si−F3 = ca. 2.02−2.25 Å). F1 and F3 occupy apical positions with a linear alignment (F1−Si−F3 = 174−179°) in a pseudo TBP structure centered at the silicon atom, while F2 occupies the equatorial position.

*General Tendency in the Solid-State Structures of **15**−**18**.* The structural parameters in **15**−**18** are shown in Tables 1 and 2, and their general trends deserve comment. The bridging fluorines (F2) in **15** and **16** and (F3) in **17** and **18** are designated as F^{br}. The Si−F^{br} bond lengths in **15**−**18** are within the distance of the minimal non-bonded approach[15] between Si and F (2.63 Å) and are comparable to the bridging Si−F bond lengths in μ-fluoro-bis(silicates) (1.700(3)−2.369(3) Å)[5b] and hexakis(fluorodimethylsilyl)benzene (2.39 Å).[5d]

The Si−F^{br} bond length is decreased upon replacing a methyl group with a phenyl group (**15** → **16**; **17** → **18**) and increasing the number of fluorine atoms (**15** → **17**; **16** → **18**).

https://doi.org/10.1021/acsomega.2c02775
ACS Omega 2022, 7, 30939−30953

Table 2. Summary of the Crystallographic and Spectroscopic Data Obtained for 17 and 18

$-SiR_{3-n}F_n$	$-SiMeF_2$ (**17a**)	$-SiMeF_2$ (**17b**)	$-SiPhF_2$ (**18a**)	$-SiPhF_2$ (**18b**)
Si−F1 [Å]	1.6300(12)	1.633(2)	1.6263(10)	1.642(5)
Si···F3 [Å]	2.2101(11)	2.2472(17)	2.1701(9)	2.021(4)
B−F3 [Å]	1.5124(19)	1.511(3)	1.5192(16)	1.568(8)
α/β [deg]	122/117	121/119	120/118	120/116
$\Sigma(C-Si-C(F^2))_3$ [deg]	354	352	353	357
% TBPe[5b]	81.0	74.6	77.8	90.5
$\delta(^{11}B)$ [ppm]	7 (br)	7 (br)	8 (br)	9 (br)
$\delta(^{19}F)$ [ppm]	−139.8 (1F), −132.3 (2F)	−138.8 (1F), −132.1 (2F)	−134.1 to −137.0 (3F)	−134.9 (3F)
$\delta(^{29}Si)$ [ppm]	−32.2	−32.8	−58.2[a]	−58.2[a]
$\Delta\delta(^{29}Si)$ [ppm]	−20.1	−20.1	−28.5[a]	−28.6[a]
$^1J_{Si-F1}$ [Hz]	276	276	273[a]	273[a]
$^1J_{Si-F2}$ [Hz]	38	39	64[a]	65[a]

[a]Observed at 181 K.

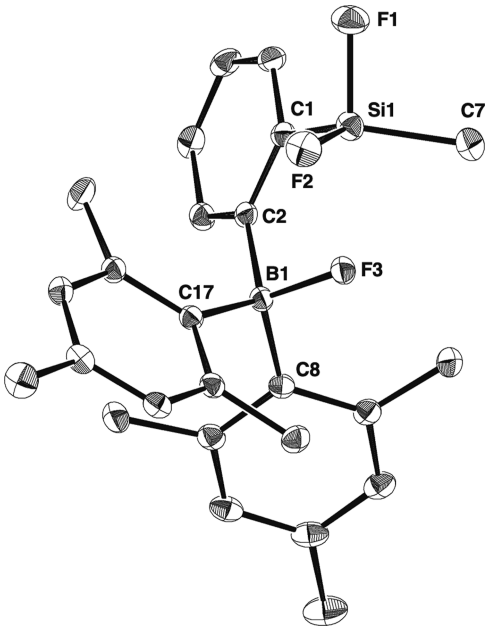

Figure 3. Crystal structure of the anionic part of **17a** (30% thermal ellipsoids).

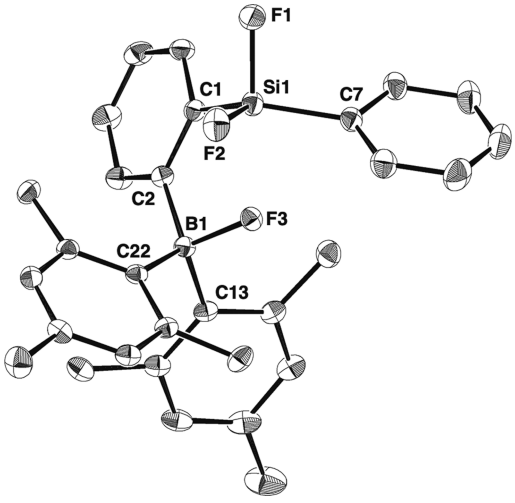

Figure 4. Crystal structure of the anionic part of **18a** (30% thermal ellipsoids).

As the Si−F^{br} bond length decreases, the sum of the bond angles between the three equatorial bonds increases and thus, the pentacoordination character (% TBP_e)[5b] of the silicon center is increased. The % TBP_e is defined as follows: [(sum of three equatorial-to-equatorial bond angles/3) − 109.5°/(120° − 109.5°)] × 100 (%)].

It was also found that the Si−F^{br} bond length is related to the in-plane angles of the C_{ipso}−Si and C_{ipso}−B bonds. When the sum of ∠Si−C1−C2 (α°) and ∠B−C2−C1 (β°) is reduced, the Si−F^{br} bond lengths in **15**−**18** are decreased, while keeping the B−F^{br} bonds intact.

The calculated %TBP_e ranges from 65.1 to 81.0 in the cryptand complexes and from 74.6 to 90.5 in the crown ether complexes.[5b] Thus, **18b** exhibits the shortest Si−F^{br} bond length (2.021(4) Å) with the largest equatorial bond angle (357°; % TBP_e = 90.5). These features are consistent with the general tendency that aryl substitution and fluoro substitution increase the Lewis acidity of the silicon center.[4,14]

It has been reported that potassium (aryl)(dialkyl)-difluorosilicates are relatively unstable and cannot be isolated even with the aid of a cryptand ligand.[14] The present *o*-borylphenyl framework enables the isolation of aryl(dialkyl)-difluorosilicates **15a** and **15b**.

Structures in Solution. *Fluorosilyl Derivatives **15** and **16**.* The structures of **15** and **16** in THF were investigated using multinuclear NMR spectroscopy. The NMR data obtained for **15** and **16** are summarized in Table 1.[16] The cryptand and crown ether complexes exhibit almost the same spectra. This indicates that **15** and **16** exist as solvent-separated ion pairs in THF solution, although **15b** forms a contact ion pair in the solid state as observed by X-ray crystallography. The ^{11}B chemical shifts (δ = 6−7) fall in the region typical for tetracoordinate borate compounds.[17] In the ^{19}F NMR spectra, the terminal fluorine (F1) is observed at δ = −145 to −147 with F−F coupling ($^2J_{F-F}$ = 9−18 Hz). On the other hand, the bridging fluorine (F2 = F^{br}) shows a broad signal at δ = −148 to −152 without F−F coupling. The coordination of the bridging fluorine to the silicon atom is reflected in the ^{29}Si NMR spectra:[18] the ^{29}Si signals are shifted upfield relative to their precursors ($\Delta\delta$ = −15 for **15** and −29 for **16**). The Si−F1 coupling constants (260 Hz for **15** and 262−266 Hz for **16**) are reduced when compared to their precursors (278 Hz for **1** and 284 Hz for **2**). The Si−F2 coupling constant of **16** (17 Hz) is larger than that of **15** (7 Hz), which corresponds to the shorter Si−F2 bond of **16** in the solid state.

https://doi.org/10.1021/acsomega.2c02775
ACS Omega 2022, 7, 30939−30953

Difluorosilyl Derivatives ***17*** *and* ***18****.* The structures of difluorosilyl derivatives **17** and **18** in THF were also investigated using multinuclear NMR spectroscopy. The NMR data are summarized in Table 2.[16] The spectra of the cryptand complexes are almost the same as those obtained for the crown ether complex. This means that **17** and **18** exist as a solvent-separated ion pair in THF, although **18b** forms a contact ion pair in the solid state. The ^{11}B chemical shifts (δ = 7 for **17** and δ = 8 for **18**) fall in the region typical for tetracoordinate borate compounds.[17] In the ^{19}F NMR spectra, the two terminal fluorine nuclei (F1 and F2) in **17** are observed at the same chemical shift (δ = −132), which is due to the rapid intramolecular exchange of the two fluorines at ambient temperature. The bridging fluorine (F3) (= F^{br}) shows a broad signal at δ = −139. On the other hand, **18** exhibits a single peak at δ = −135 due to the rapid exchange of the three fluorines (F1, F2, and F3) at ambient temperature.

The coordination of the bridging fluorine to the silicon atom is also reflected in the ^{29}Si NMR spectra:[18] (a) the ^{29}Si signals are shifted upfield relative to those of the precursors ($\Delta\delta$ = −20 for **17** and −28 for **18**); (b) the Si−F1/F2 coupling constants (276 Hz for **17** and 273 Hz for **18**) are reduced when compared to their precursors (289 Hz for **3** and 293 Hz for **4**) due to the elongation of the Si−F bonds in the pentacoordinate structures observed in the solid state; (c) the Si−F^{br} coupling constant of **18** (64 Hz at 181 K) is larger than that of **17** (38 Hz), which is consistent with the fact that the Si−F^{br} bond in **18** is shorter than that in **17** in the solid state (see Table 2).

Reaction and Structure of the *o*-Fluorosilyl Derivatives with KCN. (Fluorosilyl)borylbenzene **1** captures the cyanide ion from KCN in the presence of 18-crown-6 in toluene at room temperature (Scheme 5). The cyanide

Scheme 5. Reactions of 1 and 3 with KCN to Form 19 and 20

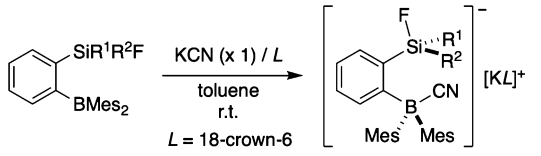

complex (**19**) was isolated as colorless crystals via recrystallization from THF.[19] (Difluorosilyl)borylbenzene **3** also captures a cyanide ion under similar reaction conditions to afford **20**.

X-ray crystallography of **19** reveals that the carbon atom in the cyanide group is bonded to the boron atom (B−CN = 1.620(8) Å), while the nitrogen atom of the cyanide ion is coordinated to the potassium cation (N···K^+ = 2.931(5) Å), as shown in Figure 5.[20] Furthermore, the potassium cation interacts with the fluorine atom of an adjacent molecule (K^+···F = 2.765(4) Å), forming an infinite chain in the solid state (see the Supporting Information).

Preparation, Reaction, and Structure of *p*-Fluorosilyl Derivatives. *p*-(Fluorosilyl)borylbenzene (**21**) was prepared for comparison with its ortho-derivative (**1**). Treating *p*-bromo(dimethylsilyl)benzene (**22**) with *tert*-BuLi at −78 °C gave aryllithium **23**, which was reacted with dimesitylfluoroborane to afford *p*-(dimethylsilyl)borylbenzene (**24**) (Scheme 6). Treating **24** with $Ph_3C^+BF_4^-$ produced **21**.[21]

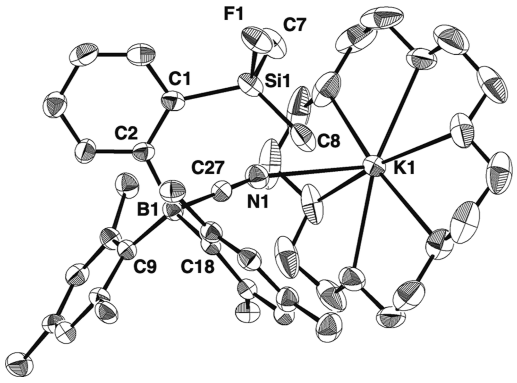

Figure 5. Crystal structure of **19** (30% thermal ellipsoids).

Scheme 6. Preparation and Reaction of *p*-Derivative 21

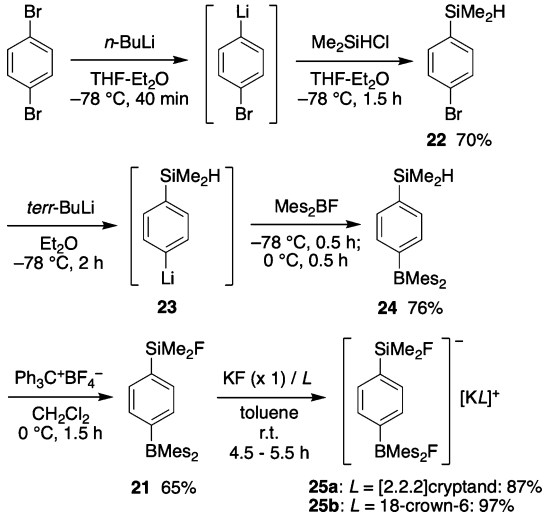

The reaction of **21** with KF in the presence of [2.2.2]-cryptand or 18-crown-6 in toluene furnished fluoroborates **25**. Cryptand complex **25a** yielded no crystals in spite of several attempts, whereas crown complex **25b** provides colorless crystals suitable for X-ray crystallography.[22] The crystal structure of **25b** revealed that fluoride F1 was coordinated to the boron atom (F1−B = 1.493(7) Å) and also interacts with the potassium cation (F1−K^+ = 2.623(3) Å), as shown in Figure 6. There are no intra- or intermolecular interactions observed between the fluorine and silicon atoms.

Competition Reactions of *o*-Fluorosilyl Derivatives. The fluoride ion affinity of fluorodimethylsilyl derivative **1** and fluorodiphenylsiyl derivative **2** were estimated using competition reactions with triarylborane **26** and (fluoro)triarylborate **27**, as shown in Scheme 7.[23,24] Mixing equimolar amounts of **1** and **27** in THF at 25 °C gave an equilibrium mixture consisting of **1**, **27**, **15b**, and **26**. The ratio of **27**/**15b** was determined to be 5:95 (K_{298} = 3.6 × 10^2) using ^{1}H NMR spectroscopy. Mixing fluorodiphenylsilyl derivative **2** and **27** in THF forms an equilibrium mixture consisting of **2**, **27**, **16b**, and **26**. The ratio of **27**/**16b** was determined to be 22:78 (K_{298} = 13). The reactions in the reverse direction were executed by mixing **15b** (or **16b**) and **26** in THF, providing almost the same equilibrium mixture (**27**/**15b** = 2:98; **27**/**16b** = 21:79). Thus, the fluorosilyl groups ortho to the boron atom increase the fluoride ion affinity of the triarylborane compounds.[3] These results suggest that the fluoride ion affinity of **1** is higher

https://doi.org/10.1021/acsomega.2c02775
ACS Omega 2022, 7, 30939−30953

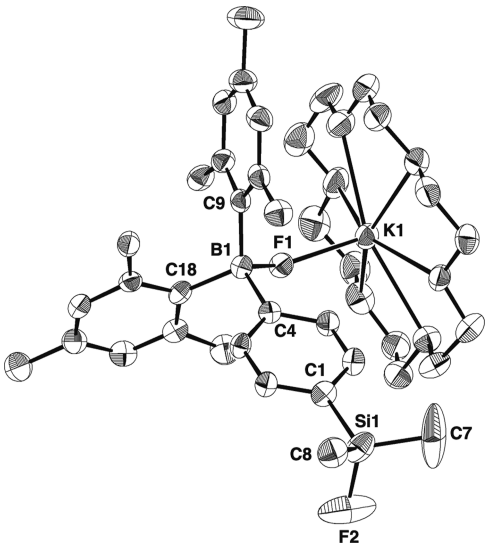

Figure 6. Crystal structure of **25b** (30% thermal ellipsoids).

Scheme 7. Competition Reactions of 1 or 2 vs 26

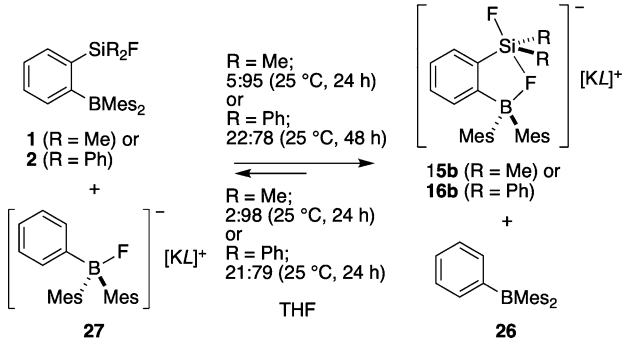

than that of **2**. In fact, competition reactions between **1** and **16b** as well as **15b** and **2** preferably form **15b** over **16b** (**15b**/**16b** = 82:18; K_{298} = 21) (Scheme 8).

Scheme 8. Competition Reactions of 1 vs 2

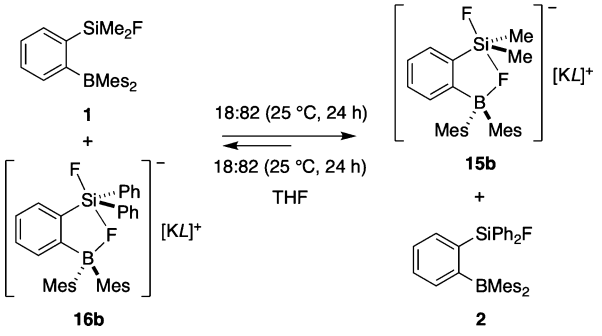

Competition Reactions of *o*-Difluorosilyl Derivatives. The fluoride ion affinity of difluorosilyl derivatives **3** and **4** was also estimated using competition reactions between fluorosilyl derivatives **1** and **2** and their corresponding fluoroborates **15b** and **16b**, as shown in Scheme 9.[23,24] Mixing equimolar amounts of **3** and **15b** in THF at 25 °C yielded an equilibrium mixture of **3**, **15b**, **17b**, and **1**. The ratio of **15b**/**17b** was determined to be 21:79 (K_{298} = 14) using ^{1}H NMR spectroscopy. Difluorophenylsilyl derivative **4** also captures a

Scheme 9. Competition Reactions of 3 or 4 vs 1

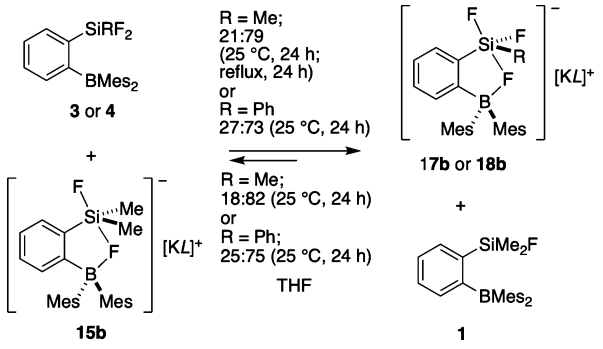

fluoride ion from **15b** to provide an equilibrium mixture of **4**, **15b**, **18b**, and **1**. The ratio of **15b**/**18b** was determined to be 27:73 (K_{298} = 7.0). The reactions in the reverse direction were carried out by mixing **17b** (or **18b**) with **1** and exhibited almost similar equilibrium positions (**17b**/**15b** = 18:82; **18b**/**15b** = 25:75). Thus, the fluoride ion affinities of difluorosilyl derivatives **3** and **4** were higher than that observed for monofluorosilyl derivative **1**. The competition reactions between **3** and **18b** as well as **17b** and **4** in THF preferably formed **17b** over **18b** (**17b**/**18b** = 55:45; K_{298} = 1.5) (Scheme 10).

Scheme 10. Competition Reactions of 3 vs 4

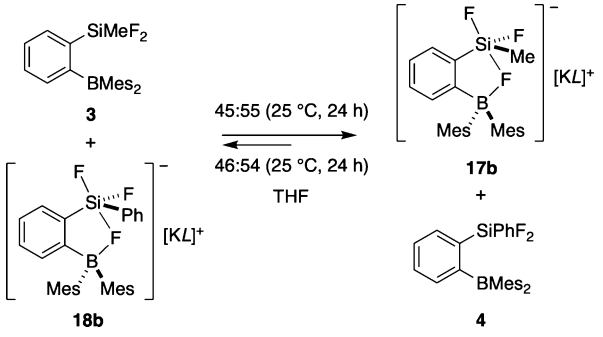

Competition Reactions of *p*-Fluorosilyl Derivatives. The fluoride ion affinity of *p*-(fluorosilyl)(boryl)benzene **21** was estimated using competition reactions with triarylborane **26** and (fluoro)triarylborate **27**, as shown in Scheme 11.[23,24] Mixing equimolar amounts of **21** and **27** in THF at 25 °C gave an equilibrium mixture of **21**, **27**, **25b**, and **26**. The ratio of **27**/**25b** was determined to be 30:70 using ^{1}H NMR spectroscopy. The reaction in the reverse direction was carried out mixing

Scheme 11. Competition Reactions of 3 or 4 vs 1

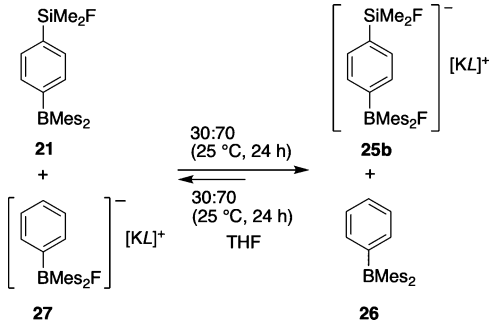

https://doi.org/10.1021/acsomega.2c02775
ACS Omega 2022, 7, 30939−30953

Chart 3. Order of Fluoride Ion Affinity Observed for 1−4 and 26

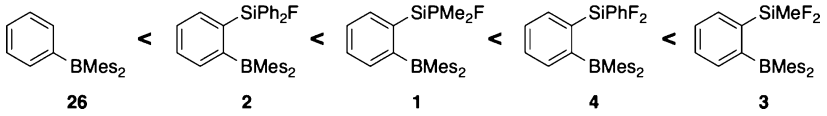

25b and 26 and provides the same equilibrium mixture. Thus, the *para* fluorosilyl group also increases the fluoride ion affinity of the triarylborane but less than the *ortho* fluorosilyl group.

Fluoride Ion Affinity of 1−4. From the results of the competition reactions, the order of the fluoride ion affinity of *o*-(silyl)borylbenzenes **1**−**4** and triarylborane **26** was determined to be **26** < **2** < **1** < **4** < **3**, as shown in Chart 3.[3a] Difluorosilyl derivatives exhibit a higher fluoride ion affinity than the monofluorosilyl derivatives. It is reasonable that the electronegative fluorine atoms increase the Lewis acidity of the silicon center. The methylsilyl derivatives exhibit a higher fluoride ion affinity than the phenylsilyl derivatives.

The total stability of *o*-(silyl)borylbenzenes **1**−**4** can be determined by the total balance between the two interactions: (a) the electrostatic attraction between the silicon center and bridging fluoride atom and (b) steric repulsion between the substituents on the silicon atom and the mesityl groups on the boron atom, which destabilize the μ-fluoro-bridged ate complex.

Computational Studies on 1−4 and 15−18. To obtain further insight into the B-μ-F−Si bonding interactions in **15**−**18**, DFT calculations,[25] GIAO calculations,[26] and natural bond orbital (NBO) analysis[27] were performed.

Since most of compounds **15**−**18** exist as separated ion pairs both in the solid state and in solution, it is reasonable that the initial coordinates were generated from the crystallographic data of the anion parts in **15a**, **16b**, **17a**, and **18a**.[28]

Geometry Optimization and GIAO NMR Shifts. We carried out the geometry optimization at the B3PW91/6-31G(d) level of theory.[25] The input coordinates were generated from the X-ray crystallographic data of the anions in **15a**, **16b**, **17a**, and **18a**. The optimized geometries were designated as $\mathbf{15}_{opt}$, $\mathbf{16}_{opt}$, $\mathbf{17}_{opt}$, and $\mathbf{18}_{opt}$ for those obtained at the B3PW91/6-31G(d) level of theory. The geometrical parameters are summarized in Table 3. Their NMR shifts were calculated using the GIAO method at the RHF/6-311+G(2d,p) level of theory.[26] The calculated geometries and NMR shifts are well matched to those observed experimentally, which is evidence for the validity of the calculations for the anion parts only.

Table 3. Calculated Structural Parameters of 15−18

	$\mathbf{15}_{opt}$	$\mathbf{16}_{opt}$	$\mathbf{17}_{opt}$	$\mathbf{18}_{opt}$
Si−F^{ap} [Å]	1.664	1.668	1.653	1.655
Si−F^{eq} [Å][a]			1.620	1.619
Si···F^{br} [Å][a]	2.508	2.355	2.273	2.175
B−F^{br} [Å][a]	1.488	1.510	1.508	1.528
α/β [deg][a]	124.3/120.1	123.5/119.2	121.9/118.1	120.7/117.6
$\delta(^{29}Si)$ [ppm][b]	4.7	−28.6	−36.9	−61.3
$\delta(^{11}B)$ [ppm][b]	3.8	4.9	4.8	6.3
$\delta(^{19}F)$ [ppm][b]	−146.3	−148.8	−135.7	−137.6
	−143.5	−126.1	−135.6	−131.1
			−131.1	−114.3

[a]Optimized at B3PW91/6-31G(d). [b]GIAO at RHF/6-311+G-(2d,p)//B3PW91/6-31G(d).

NBO Analysis. In order to shed light on the bonding interactions in **15**−**18**, NBO analysis was executed at the B3PW91/6-31G(d) level of theory.[27] F^{ap} corresponds to F1 in **15**, **16**, **17**, and **18**; F^{eq} corresponds to F2 in **17** and **18**; F^{br} corresponds to F2 in **15** and **16** and F3 in **17** and **18**.

The second-order perturbation theory analysis reveals intramolecular coordination from the donor LP_F to the acceptor LP^*_{Si}. The sum of the stabilization energy $E(2)$ was calculated to be 18−31 kcal/mol, as shown in Table 4. One of the lone pairs of the bridging fluorine atom (LP[F]) mainly coordinates to the σ^*(Si−F) orbital (LP*[Si]).

Table 4. Selected NBO Analysis Data of 15−18[a]

donor NBO[b]	acceptor NBO[c]	E(2)[d](kcal/mol)
	$\mathbf{15}_{opt}$	
LP(1)[F4]	LP*(1)[Si]	4.88
LP(3)[F4]	LP*(1)[Si]	13.84
	$\mathbf{16}_{opt}$	
LP(1)[F4]	LP*(1)[Si]	5.86
LP(3)[F4]	LP*(1)[Si]	23.24
	$\mathbf{17}_{opt}$	
LP(1)[F3]	LP*(2)[Si]	5.34
LP(3)[F3]	LP*(2)[Si]	23.12
	$\mathbf{18}_{opt}$	
LP(3)[F5]	LP*(2)[Si]	31.27

[a]Optimized at B3PW91/6-31G(d). [b]LP[F] = lone pair at the bridging fluorine atom. [c]LP*[Si] = vacant orbital at the silicon atom. [d]Stabilization energy associated with the delocalization of electrons from LP[F] to LP*[Si] according to second-order perturbation theory analysis of the fock matrix in NBO basis. The threshold for listing is 5.0 kcal/mol.

Computed Fluoride Ion Affinity. In order to assess the strength of the interactions involving the bridging fluoride in **15**−**18**, we have computed the gas-phase fluoride ion affinities (FIAs) of **1**−**4**.[4h,29] COF_2 was used as a reference compound to simplify the calculations (Scheme 12). The resulting relative FIAs were converted to an absolute scale using the experimentally known value (49.9 kcal/mol) for the FIA of COF_2. The obtained FIAs are as follows: −81.1 kcal/mol for **1**, −80.2 kcal/mol for **2**, −81.1 kcal/mol for **3**, −84.2 kcal/mol

Scheme 12. Isodesmic Reactions for FIA Calculations of 1, 2, 3, and 4

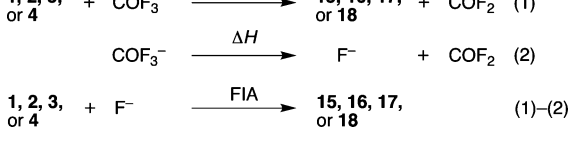

https://doi.org/10.1021/acsomega.2c02775
ACS Omega 2022, 7, 30939−30953

for **4**, and −72.5 kcal/mol for **26** (see the Supporting Information). Thus, the order of the calculated FIAs is **4** > **3** > **1** > **2** > **26**. The calculated order is partly inconsistent with the observed one: the order of **3** and **4** is reversed. Although the reason is not clear, it may be plausible that the competition reactions of **3** versus **4** did not completely achieve the equilibria or the effect of the countercation cannot be negligible.

Dynamic Behavior of μ-Fluoro-Bridged Ate Complexes 15−18: Site-Exchange Process Monitored Using ^{19}F NMR Spectroscopy. The site exchange between the two or three fluorine atoms in **15**−**18** was observed using variable-temperature ^{19}F NMR spectroscopy. The changes in the NMR spectra can be rationalized using four processes described below.[5b]

General Outline of the Site-Exchange Processes. *Process a: Rotation around the Si−C_{ipso} Bond.* Rotation around the Si−C_{ipso} bond causes site exchange between F^{ap} and F^{eq}, resulting in the coalescence of the peaks observed for F^{ap} and F^{eq}. This rotation is retarded with an increase in the strength of the Si−F^{br} bond.

Process b: F^{br} Migration between the Boron and Silicon Atoms. The migration of F^{br} between the boron and silicon atoms results in the formation of tetracoordinate boron (fluoroborate) or pentacoordinate silicon (fluorosilicate), resulting in the broadening of the peak corresponding to F^{br}. The B−F^{br} bond is strong when compared to the Si−F^{br} bond (interaction), as observed in the crystal structures. Thus, F^{br} migration may be a high-energy process when compared to Si−C_{ipso} bond rotation.

Process c: Pseudorotation at the Pentacoordinate Silicon Center. Pseudorotation[3c,d] at the pentacoordinate silicon causes site exchange among F^{ap}, F^{eq}, and F^{br}, resulting in the coalescence of these peaks.

Process d: Flipping of the Five-Membered Ring. Flipping of the C−Si−μ-F−Si−C five-membered ring in the *o*-bis(silyl)benzene complex has been discussed by Tamao et al.[5b] However, flipping of the C−Si−μ-F−B−C five-membered ring in the *o*-(silyl)borylbenzene complexes may not cause large motion because the five-membered ring is only slightly puckered.

FMe_2Si Derivatives 15. Two peaks corresponding to F^{ap} (=F1) (δ = −147) and F^{br} (=F2) (δ = −152) were observed at 298 K (Figures S2−S5, see the Supporting Information).[9] These peaks exhibit no noticeable change up to 383 K.

FPh_2Si Derivatives 16. Two distinct peaks corresponding to F^{ap} (=F1) (δ = −145) and F^{br} (=F2) (δ = −148) were observed at 298 K in DMSO-d_6 (Figure S2-S6, see the Supporting Information).[9] These peaks broadened with increasing temperature and then coalesced at 361 K. The peaks finally appeared as a single peak at 373 K. This was attributed to F^{br} migration from the boron to silicon atoms (process b) and subsequent pseudorotation of the resulting pentacoordinate silicon (process c), as shown in Scheme 13. The two processes may occur coincidentally in the same temperature range. The possibility of rotation around the Si−C_{ipso} bond (process a) rather than pseudorotation cannot be excluded because the two processes lead to the same structure in **16**.

F_2MeSi Derivatives 17. Three peaks corresponding to F^{ap} (=F1) (δ = −125.9), F^{eq} (=F2) (δ = −137.0), and F^{br} (=F3) (δ = −138.8) were observed at 193 K in THF-d_8, as shown in Figure 7a. Increasing the temperature broadened the two peaks

Scheme 13. Plausible F−F Exchange Process between B and Si for 15 and 16: (b) F^- Migration between B and Si; (c) Pseudorotation at Si

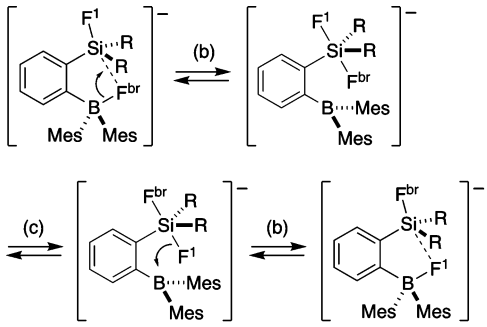

(b) F^- migration between B and Si, (c) pseudorotation at Si

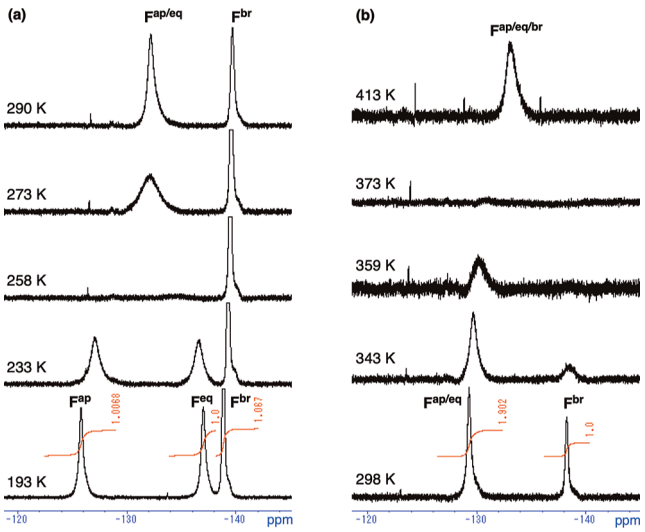

Figure 7. Variable-temperature ^{19}F NMR spectra of **17a** recorded (a) at lower temperatures in THF-d_8 and (b) at higher temperatures in DMSO-d_6.

corresponding to F^{ap} and F^{eq}, which then coalesce at 258 K, while the F^{br} peak remained unchanged. This was attributed to the site exchange between F^{ap} and F^{eq} caused by Si−C_{ipso} bond rotation (process a). The combined peak corresponding to $F^{ap/eq}$ (δ = −132) and F^{br} (δ = −138) was observed at 290 K. As shown in Figure 7b, increasing the temperature broadened the $F^{ap/eq}$ and F^{br} peaks, which then coalesce at 373 K and finally appear as a single peak at 413 K. This was attributed to site exchange among F^{ap}, F^{eq}, and F^{br} caused by F^{br} migration (process b) from boron to silicon and subsequent pseudorotation (process c) of the resulting pentacoordinate silicon, as shown in Scheme 14. It is notable that the F^{br} peak was completely broadened prior to its coalescence at 359 K, which indicates that F^{br} migration and pseudorotation occur in a stepwise manner.

F_2PhSi Derivatives 18. The dynamic behavior of F_2PhSi derivatives **18** was rather complicated. The NMR spectra recorded in THF-d_8 at 181 K showed two sets of peaks in a 2:1 ratio (Figure 8). On the base of the peak intensities, we tentatively assigned the peaks at δ −123.4 (dd, J_{F-F} = 30 and 15 Hz, F^{ap}(maj)), −135.8 (broad, F^{br}(maj)), and −146.9 (t, J_{av} = 33 Hz, F^{eq}(maj)) to major isomer $\mathbf{18}_{maj}$ and the peaks at δ −128.7 (dd, J_{F-F} = 23 and 11 Hz, F^{ap}(min)), −139.1 (broad,

https://doi.org/10.1021/acsomega.2c02775
ACS Omega 2022, 7, 30939−30953

Scheme 14. Plausible F−F Exchange Process between B and Si for 17 and 18: (a) Si−C Rotation, (b) F^- Migration between B and Si, and (c) Pseudorotation at Si

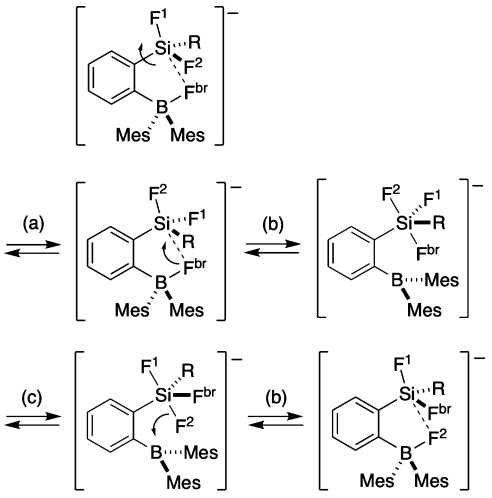

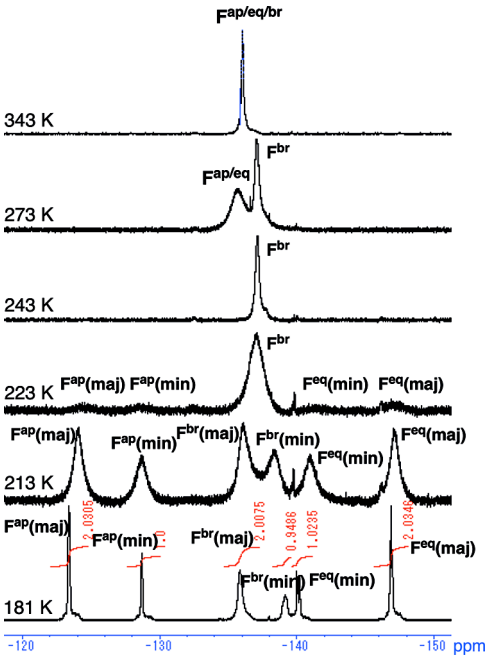

Figure 8. Variable-temperature ^{19}F NMR spectra of **18a** recorded in THF-d_8.

F^{br}(min)), and −140.1 (dd, J = 65 and 25 Hz, F^{eq}(min)) to minor isomer $\mathbf{18}_{min}$.

Increasing the temperature led to line broadening and coalescence of the peaks. F^{br}(maj) and F^{br}(min) coalesced at 223 K. At that temperature, F^{ap}(maj), F^{eq}(maj), F^{ap}(min), and F^{eq}(min) underwent massive broadening and then appeared as a single peak ($F^{ap/eq}$) at 273 K. Finally, $F^{br}$and $F^{ap/eq}$ coalesced to a single peak ($F^{ap/eq/br}$) at 343 K. It was confirmed that these behaviors were reversible between 181 and 343 K.

The two isomers $\mathbf{18}_{maj}$ and $\mathbf{18}_{min}$ may be assignable to conformational isomers associated to the flipping of the C−Si−μ-F−B−C five-membered ring. The optimized structures of the two isomers were obtained at the B3PW91/6-31G(d) level of theory, as shown in Scheme 15 (see the Supporting Information in detail). The flipping causes change in the

Scheme 15. Plausible Flipping of the Puckered C−Si−μ-F−B−C Five-Membered Ring in $\mathbf{18}_{maj}$ and $\mathbf{18}_{min}$ (above) and Their Optimized Structures at the B3PW91/6-31G(d) Level of Theory (below)

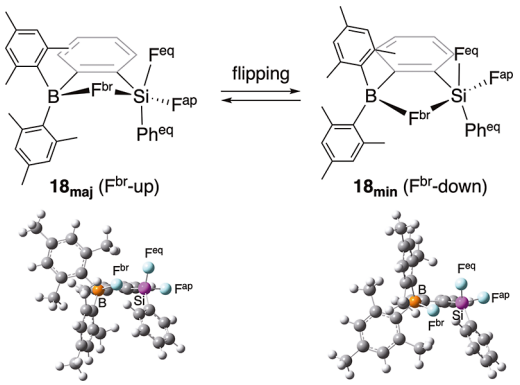

conformations of the two Mes groups on the boron atom. Thus, one of the Mes groups and the Ph group on the silicon atom are almost parallel to each other in more stable $\mathbf{18}_{maj}$, whereas the Mes group and the Ph group are perpendicular to each other, which causes the steric repulsion, in less stable $\mathbf{18}_{min}$. It was found that $\mathbf{18}_{min}$ is the same as $\mathbf{18}_{opt}$ in terms of the geometrical parameters and the thermal parameters.

The calculated energy difference between $\mathbf{18}_{maj}$ and $\mathbf{18}_{min}$ (ΔG°_{181}) is 0.184 kcal/mol, and the derived equilibrium constant K is 1.67, which is close to the observed ratio of the two isomers at 181 K (2:1). The unusual behavior of **18a** remains unclear and still under investigation.

CONCLUSIONS

A series of *o*-(fluorosilyl)(boryl)benzenes **1**−**4** were prepared using [*o*-(silyl)phenyl]lithium anions **7**, **8**, **11**, and **12** and characterized using NMR spectroscopy and X-ray crystallography. Compounds **1**−**4** capture a fluoride ion in the presence of [2.2.2]cryptand or 18-crown-6 to afford their corresponding μ-fluoro-bridged ate complexes (**15**−**18**), which were also characterized in solution and the solid state. DFT studies and NBO analysis of **15**−**18** revealed the nature of the Si−F and B−F bonding interactions in the μ-fluoro-bridges. The fluoride ion affinities of **1**−**4** were demonstrated using competitive reactions, and the order of the fluoride ion affinity was determined to be **3** > **4** > **1** > **2**. The dynamic behavior of **15**−**18** at variable temperatures mainly consists of (a) rotation around the Si−C_{ipso} bond, (b) F^{br} migration between the boron and silicon atoms, and (c) pseudorotation at the pentacoordinate silicon center.

EXPERIMENTAL SECTION

General Procedures. ^1H (400 MHz), ^{11}B (128.3 MHz), ^{13}C (100 MHz), ^{19}F (376 MHz), and ^{29}Si (79.4 MHz) NMR spectroscopy was recorded on a JEOL EX-400 or AL-400 spectrometer. The ^1H and ^{13}C NMR chemical shifts were referenced to the residual NMR solvent signal ($CDCl_3$: $\delta(^1H)$ = 7.26 ppm, $\delta(^{13}C)$ = 77.0 ppm; C_6D_6: $\delta(^1H)$ = 7.20 ppm, $\delta(^{13}C)$ = 128.0 ppm). The ^1H and ^{13}C chemical shifts in THF-d_8 were referenced to tetramethylsilane as an internal standard ($\delta(^1H)$ = 0 ppm; $\delta(^{13}C)$ = 0 ppm). The ^{11}B chemical shifts

https://doi.org/10.1021/acsomega.2c02775
ACS Omega 2022, 7, 30939−30953

were referenced to $BF_3{\cdot}Et_2O$ as an external standard (δ = 0 ppm). The ^{19}F chemical shifts were referenced to $CFCl_3$ as an external standard (δ = 0 ppm). The ^{29}Si chemical shifts were referenced to tetramethylsilane as an external standard (δ = 0 ppm). Mass spectroscopy (EI) was recorded at 70 eV using a JEOL SX-102A mass spectrometer located at the Natural Science Center for Basic Research and Development (N-BARD), Hiroshima University. Melting points were measured using a Yanaco micro melting point apparatus and were uncorrected. Elemental analysis was performed on a PerkinElmer 2400CHN elemental analyzer located at Prof. Yamamoto's Laboratory. Column chromatography on silica gel was performed using Kieselgel 60 (230−400 mesh) (Merck). All reactions were carried out under an inert gas atmosphere otherwise noted.

Hexane was distilled under a nitrogen atmosphere over calcium hydride, or the dehydrated solvent (<10 ppm; Kanto Chemical Co., Inc.) was dried using a solvent dispensing system (GlassContour) under a nitrogen atmosphere (99.999%). THF and Et_2O were distilled under a nitrogen atmosphere over sodium diphenylketyl, or the dehydrated solvents (<10 ppm for THF and <50 ppm for Et_2O; Kanto Chemical Co., Inc.) were dried using a solvent dispensing system (GlassContour) under a nitrogen atmosphere (99.999%). THF-d_8, toluene, and benzene were distilled under a nitrogen atmosphere over sodium diphenylketyl. CCl_4, $CHCl_3$, CH_2Cl_2, CH_3CN, and MeOH were distilled under a nitrogen atmosphere over calcium hydride.

The following reagents were used as received: *tert*-BuLi in pentane (Kanto Chemical Co., Inc), *n*-BuLi in hexane (Kanto Chemical Co., Inc.), [2.2.2]cryptand (Wako Pure Chemical Industries, Ltd.), 1,2-dibromobenzene (Tokyo Chemical Industry Co., Ltd.), 1,4-dibromobenzene (Sigma-Aldrich), HF·pyridine (Tokyo Chemical Industry Co., Ltd.), AgF (Mitsuwa Chemicals Co., Ltd.), CuF_2 (98%) (Sigma-Aldrich), $PdCl_2$ (Wako Pure Chemical Industries, Ltd.), KCN (Katayama), KCI (Wako Pure Chemical Industries, Ltd.), BCl_3 in heptane (Sigma-Aldrich), BCl_3 in CH_2Cl_2 (Wako Pure Chemical Industries, Ltd.), chloro(dimethoxy)methylsilane (Shin-Etsu Chemical Co., Ltd.), trimethylphenylsilane (Shin-Etsu Chemical Co., Ltd.), chlorotrimethylsilane (Tokyo Chemical Industry Co., Ltd.), chlorodimethylsilane (Tokyo Chemical Industry Co., Ltd.), and phenylsilane (Tokyo Chemical Industry Co., Ltd.).

KF (spray-dried grade (98%)) (Wako Pure Chemical Industries, Ltd.) was dried in vacuo at 150 °C for 1 d. $BF_3{\cdot}OEt_2$ (Kanto Chemical Co., Inc.) was distilled over CaH_2. $B(OMe)_3$ (Tokyo Chemical Industry Co., Ltd.) was distilled under a nitrogen atmosphere. Ph_3CBF_4 (Sigma-Aldrich) was recrystallized from CH_3CN and dried in vacuo. *n*-Bu_4NCl (Tokyo Chemical Industry Co., Ltd.) was recrystallized from acetone and dried in vacuo. *n*-Bu_4NBr (Sigma-Aldrich) was recrystallized from ethyl acetate and dried in vacuo. *n*-Bu_4NI (Tokyo Chemical Industry Co., Ltd.) was recrystallized from ethyl acetate and dried in vacuo. 18-crown-6 (Tokyo Chemical Industry Co., Ltd.) was recrystallized from CH_3CN and dried in vacuo. 12-Crown-4 (Merck) was distilled under a nitrogen atmosphere over CaH_2.

Fluorodimesitylborane[30] and dimesitylphenylborane[31] (**26**) were prepared according to previously reported procedures. The preparation of compounds **1**, **2**, **13**, and **14** has been reported in our previous papers.[9,10]

Synthetic Procedures. *o-[(Difluoromethylsilyl)](dimesitylboryl)benzene (**3**).* HF·pyridine (65% HF, 2.0 mL) was added dropwise via a plastic syringe to a solution of **13** (1.08 g, 2.51 mmol) in Et_2O (7.5 mL) in a plastic container at 0 °C, and the resulting reaction mixture was stirred at 0 °C for 1 h. The solvent was evaporated, and the residue was dissolved in hexane (10 mL). The resulting solution was filtered through a membrane filter; the filtrate was partly concentrated and cooled to −18 °C to give **3** as a white solid (850 mg, 84%).

mp 111−113 °C (decomposed/sealed). ^1H NMR (THF-d_8): δ −0.24 (t, $^3J_{F-H}$ = 7 Hz, 3H), 1.51−2.33 (br, 18H), 6.80 (br, 4H), 7.35 (d, ^3J = 7 Hz, 1H), 7.49 (d of quint., ^3J = 7 Hz, ^4J = 2 Hz, 2H), 7.81 (dd, ^3J = 6 Hz, ^4J = 2 Hz, 1H). ^{13}C NMR (THF-d_8): δ −3.9 (t, $^2J_{F-C}$ = 18 Hz, CH_3), 21.4 (CH_3), 22.5−23.5 (br, CH_3), 24.2 (br, CH_3), 128.5−130.1 (br, CH), 130.3 (CH), 131.9 (CH), 134.9 (CH), 135.8 (C), 136.0 (C), 136.1 (t, $^3J_{F-C}$ = 4 Hz, CH), 136.2 (C), 139.6−144.5 (m, C), 157.4 (C). ^{11}B NMR (THF-d_8): δ 75 (br). ^{19}F NMR (THF-d_8): δ −133.1 (s), −128.9 (s). ^{29}Si NMR (THF-d_8): δ −12.1 (t, $^1J_{Si-F}$ = 293 Hz). Anal. Calcd for $C_{25}H_{29}BF_2Si$: C, 73.89; H, 7.19. Found: C, 73.79; H, 7.40.

*o-[(Difluorophenylsilyl)](dimesitylboryl)benzene (**4**).* This compound was prepared using the same procedure described for **3** from **14** (591 mg, 1.20 mmol) and HF·pyridine (65% HF, 0.6 mL) and obtained as a white solid (345 mg, 0.74 mmol) in 61% yield.

mp 136−139 °C (decomposed/sealed). ^1H NMR (THF-d_8): δ 0.67−2.56 (br, 18H), 5.73−6.95 (br, 4H), 7.15 (dd, ^3J = 8 Hz, ^4J = 1 Hz, 2H), 7.22 (t, ^3J = 8 Hz, 2H), 7.36−7.43 (m, 2H), 7.50−7.61 (m, 2H), 8.00 (d, ^3J = 8 Hz, 1H). ^{13}C NMR (THF-d_8): δ 21.4 (CH_3), 22.5−23.7 (br, CH_3), 24.2 (CH_3), 128.3 (CH), 128.5−129.9 (br, CH), 129.5 (t, $^2J_{C-F}$ = 20 Hz, C), 130.3 (CH), 131.5 (CH), 132.3 (CH), 133.4 (C), 133.6 (C), 133.7 (t, $^3J_{F-C}$ = 2 Hz, CH), 133.8 (C), 135.3 (CH), 137.2 (t, $^3J_{F-C}$ = 3 Hz, CH), 139.5−144.6 (m, C), 157.8 (C). ^{11}B NMR (THF-d_8): δ 75 (br). ^{19}F NMR (THF-d_8): δ −139.8 (d, $^2J_{F-F}$ = 16 Hz), −132.4 (d, $^2J_{F-F}$ = 17 Hz). ^{29}Si NMR (THF-d_8): δ −29.7 (t, $^1J_{Si-F}$ = 293 Hz). Anal. Calcd for $C_{30}H_{31}BF_2Si$: C, 76.92; H, 6.67. Found: C, 77.31; H, 7.03.

*Potassium 18-Crown-6 [o-(Fluorodimethylsilyl)phenyl]-fluorodimesitylborate (**15b**).* A solution of **1** (202 mg, 0.50 mmol), 18-crown-6 (136 mg, 0.51 mmol), and KF (30 mg, 0.51 mmol) in toluene (1.5 mL) was stirred at room temperature for 5 h forming a white precipitate. The solvent was removed in vacuo, and the resulting white solid was dissolved in a minimum amount of THF at room temperature. A small amount of hexane was then slowly added over the saturated solution, resulting in a two-layer solution. The two-layer solution was allowed to stand at room temperature for 1 d to give **15b**·THF (332 mg, 83% yield) as colorless crystals.

mp 155−157 °C (decomposed). ^1H NMR (THF-d_8): δ 0.05 (br, 6H), 1.87 (br, 12H), 2.08 (s, 6H), 3.53 (s, 24H, *crown*), 6.36 (br, 4H), 6.78−6.80 (m, 2H), 7.05−7.08 (m, 1H), 7.60−7.62 (m, 1H). ^{13}C NMR (THF-d_8): δ 2.7 (br), 21.2, 26.3, 71.1 (*crown*), 122.7, 127.2, 128.6, 130.9, 133.3 (d, $^3J_{F-C}$ = 8 Hz), 134.0 (d, $^3J_{F-C}$ = 9 Hz), 141.6 (dd, $^2J_{F-C}$ = 15 Hz, $^2J_{F-C}$ = 7 Hz), 142.0 (br); the peaks corresponding to the *ipso* and *para* carbon atoms in the mesityl groups were not observed. ^{11}B NMR (THF-d_8): δ 6 (br). ^{19}F NMR (THF-d_8): δ −151.7 (br), −146.6 (d of sept, $^3J_{F-H}$ = 9 Hz, $^2J_{F-F}$ = 9 Hz). ^{29}Si NMR (THF-d_8): δ 6.4 (d, $^1J_{Si-F}$ = 260 Hz). Anal. Calcd for $C_{42}H_{64}BF_2KO_7Si$ (**15b**·THF): C, 63.30; H, 8.09. Found: C, 63.02; H, 8.45.

https://doi.org/10.1021/acsomega.2c02775
ACS Omega 2022, 7, 30939−30953

*Potassium [2.2.2]Cryptand [o-(fluorodimethylsilyl)-phenyl]fluorodimesitylborate (**15a**).* This compound was prepared using the same procedure described for **15b** from **1** (206 mg, 0.51 mmol), KF (30 mg, 0.51 mmol), and [2.2.2]cryptand (188 mg, 0.50 mmol) and obtained as colorless crystals of **15a**·THF (340 mg, 0.37 mmol) in 75% yield.

mp 185−187 °C (decomposed). ^{1}H NMR (THF-d_8): δ 0.05 (br, 6H), 1.87 (br, 12H), 2.09 (s, 6H), 2.50 (t, J = 5 Hz, 12H, *cryptand*), 3.47 (t, J = 5 Hz, 12H, *cryptand*), 3.51 (s, 12H, *cryptand*), 6.37 (br, 4H), 6.81−6.83 (m, 2H), 7.07−7.09 (m, 1H), 7.62−7.74 (m, 1H). ^{13}C NMR (THF-d_8): δ 2.7 (br), 21.2, 26.3, 54.6 (*cryptand*), 68.3 (*cryptand*), 71.2 (*cryptand*), 122.8, 127.3, 128.7, 130.9, 133.4 (d, $^{3}J_{F-C}$ = 7 Hz), 134.0 (d, $^{3}J_{F-C}$ = 7 Hz), 141.6 (dd, $^{2}J_{F-C}$ = 15 Hz, $^{2}J_{F-C}$ = 7 Hz), 142.0 (br); the peaks corresponding to the *ipso* and *para* carbon atoms in the mesityl groups were not observed. ^{11}B NMR (THF-d_8): δ 6 (br). ^{19}F NMR (THF-d_8): δ −151.9 (br), −146.8 (d of sept, $^{3}J_{F-H}$ = 9 Hz, $^{2}J_{F-F}$ = 9 Hz). ^{29}Si NMR (THF-d_8): δ 6.5 (dd, $^{1}J_{Si-F}$ = 260 Hz, $^{1}J_{Si-F}$ = 7 Hz). Anal. Calcd for $C_{48}H_{76}BF_2KN_2O_7Si$ (**15a**·THF): C, 63.41; H, 8.43; N, 3.08. Found: C, 63.71; H, 8.49; N, 3.13.

*Potassium [2.2.2]Cryptand [o-(fluorodiphenylsilyl)-phenyl]fluorodimesitylborate (**16a**).* This compound was prepared using the same procedure described for **15b** from **2** (263 mg, 0.50 mmol), KF (30 mg, 0.51 mmol), and [2.2.2]cryptand (189 mg, 0.50 mmol) and obtained as colorless crystals of **16a**·2THF in 80% yield. One free molecule of H_2O was included in the unit cell of the crystals when the recrystallization step was performed in the air.

mp 100−101 °C (decomposed). ^{1}H NMR (THF-d_8): δ 1.63 (br, 12H), 2.01 (s, 6H), 2.50 (t, J = 5 Hz, 12H, *cryptand*), 3.48 (t, J = 5 Hz, 12H, *cryptand*), 3.52 (s, 12H, *cryptand*), 6.16 (br, 4H), 6.86−6.97 (m, 9H), 7.14 (d, J = 7 Hz, 1H), 7.72 (d, J = 7 Hz, 4H), 8.07 (d, J = 7 Hz, 1H). ^{13}C{^{1}H} NMR (THF-d_8): δ 21.0, 26.2, 54.4 (*cryptand*), 68.1 (*cryptand*), 71.0 (*cryptand*), 123.0, 126.2, 127.2, 127.7, 128.4, 130.8, 133.8−133.9 (m), 134.8−134.9 (m), 136.1 (t, $^{2}J_{F-C}$ = 4 Hz), 138.3−138.6 (m), 141.5 (br), 153.8 (br), 172.5 (br); 13 signals were found for the 14 non-equivalent aromatic carbon atoms. ^{11}B{^{1}H} NMR (THF-d_8): δ 7 (br). ^{19}F NMR (THF-d_8, 193 K, δ): −148.1 (br), −144.9 (d, $^{2}J_{F-F}$ = 18 Hz). ^{29}Si{^{1}H} NMR (THF-d_8): δ −32.6 (dd, $^{1}J_{Si-F}$ = 266 Hz and $^{1}J_{Si-F}$ = 17 Hz). Anal. Calcd for $C_{54}H_{74}BN_2O_7F_2SiK$ (**16a**·H_2O): C, 66.24; H, 7.62; N, 2.86. Found: C, 66.49; H, 7.67; N, 2.77.

*Potassium 18-Crown-6 [o-(Fluorodiphenylsilyl)phenyl]-fluorodimesitylborate (**16b**).* This compound was prepared using the same procedure described for **15b** and obtained as colorless crystals of **16b**·2THF in 85% yield.

mp 168−169 °C (decomposed). ^{1}H NMR (THF-d_8): δ 1.62 (br, 12H), 2.01 (s, 6H), 3.53 (s, 24H, *crown*), 6.16 (br, 4H), 6.86−6.97 (m, 8H), 7.13 (d, J = 7 Hz, 1H), 7.72 (d, J = 7 Hz, 4H), 8.07 (d, J = 7 Hz, 1H). ^{13}C{^{1}H} NMR (THF-d_8): δ 21.2, 26.4, 71.1 (*crown*), 123.1, 126.4, 127.4, 127.8, 128.6, 129.0, 131.1, 134.0−134.1 (m), 135.0−135.1 (m), 136.3 (t, $^{2}J_{F-C}$ = 4 Hz), 138.5−138.8 (m), 141.6 (br), 154.1 (br); 13 signals were found for the 14 non-equivalent aromatic carbon atoms. ^{11}B{^{1}H} NMR (THF-d_8): δ 7 (br). ^{19}F NMR (THF-d_8, 193 K): δ −148.0 (br), −144.9 (d, $^{2}J_{F-F}$ = 18 Hz). ^{29}Si{^{1}H} NMR (THF-d_8): δ −32.7 (dd, $^{1}J_{Si-F}$ = 262 Hz, $^{1}J_{Si-F}$ = 17 Hz). Anal. Calcd for $C_{56}H_{76}BO_8F_2SiK$ (**16b**·2THF): C, 67.72; H, 7.71. Found: C, 67.35; H, 7.81.

*Potassium [2.2.2]Cryptand [o-(Difluoromethylsilyl)-phenyl]fluorodimesitylborate (**17a**).* This compound was prepared using the same procedure described for **15b** from **3** (163 mg, 0.40 mmol), KF (26 mg, 0.44 mmol), and [2.2.2]cryptand (169 mg, 0.44 mmol) and obtained as colorless crystals of **17a**•THF (303 mg, 0.36 mmol) in 90% yield.

mp 219−223 °C (sealed). ^{1}H NMR (THF-d_8): δ −0.13 (dt, $^{3}J_{F-H}$ = 9 Hz, $^{3}J_{F-H}$ = 6 Hz, 3H), 1.88 (s, 12H), 2.09 (s, 6H), 2.54 (t, ^{3}J = 5 Hz, 12H, *cryptand*), 3.52 (t, ^{3}J = 5 Hz, 12H, *cryptand*), 3.56 (s, 12H, *cryptand*), 6.39 (s, 4H), 6.85 (ddd, ^{3}J = 7 Hz, ^{4}J = 2 Hz, 1H), 6.91 (ddd, ^{3}J = 7 Hz, ^{4}J = 2 Hz, 1H), 7.17 (d, ^{3}J = 8 Hz, 1H), 7.68 (dd, ^{3}J = 7 Hz, ^{4}J = 2 Hz, 1H). ^{13}C NMR (THF-d_8): δ 0.7 (q, $^{2}J_{F-C}$ = 22 Hz, CH_3), 21.3 (CH_3), 25.6 (d, $^{4}J_{F-C}$ = 3 Hz, CH_3), 54.7 (*cryptand*, CH_2), 68.4 (*cryptand*, CH_2), 71.3 (*cryptand*, CH_2), 123.1 (CH), 128.7 (CH), 128.9 (CH), 131.5 (C), 134.0 (d, $^{3}J_{F-C}$ = 8 Hz, CH), 134.6 (d, $^{3}J_{F-C}$ = 2 Hz, CH), 136.6 (d, $^{2}J_{F-C}$ = 17 Hz, C), 141.9 (C), 153.8 (br, C), 173.0 (br, C). ^{11}B NMR (THF-d_8): δ 7 (br). ^{19}F NMR (THF-d_8): δ −139.8 (br), −132.3 (br). ^{29}Si NMR (THF-d_8): δ −32.2 (ddd, $^{1}J_{Si-F}$ = 276 Hz, $^{1}J_{Si-F}$ = 38 Hz). Anal. Calcd for $C_{47}H_{73}BF_3KN_2O_7Si$ (**17a**·THF). Anal. Calcd for C, 61.82; H, 8.06; N, 3.07. Found: C, 61.81; H, 8.20, N 3.26.

*Potassium 18-Crown-6 [o-(Difluoromethylsilyl)phenyl]-fluorodimesitylborate (**17b**).* This compound was prepared using the same procedure described for **15b** and obtained as colorless crystals of **17b**•2THF in 93% yield.

mp 172−175 °C (decomposed/sealed). ^{1}H NMR (THF-d_8): δ −0.13 (q, $^{3}J_{F-H}$ = 7 Hz, 3H), 1.88 (s, 12H), 2.09 (s, 6H), 3.58 (s, 24H, *crown*), 6.39 (s, 4H), 6.85 (ddd, ^{3}J = 7 Hz, ^{4}J = 2 Hz, 1H), 6.91 (ddd, ^{3}J = 7 Hz, ^{4}J = 2 Hz, 1H), 7.17 (d, ^{3}J = 7 Hz, 1H), 7.68 (dq, ^{3}J = 8 Hz, ^{4}J = 1 Hz, 1H). ^{13}C NMR (THF-d_8): δ 0.6 (q, $^{2}J_{F-C}$ = 22 Hz, CH_3), 21.2 (CH_3), 26.4 (CH_3), 71.1 (*crown*, CH_2), 123.1 (CH), 128.6 (CH), 128.8 (CH), 131.5 (C), 134.0 (d, $^{3}J_{F-C}$ = 5 Hz, CH), 134.6 (q, $^{3}J_{F-C}$ = 3 Hz, CH), 136.5 (d, $^{2}J_{F-C}$ = 17 Hz, C), 141.8 (C), 153.7 (br, C), 172.9 (br, C). ^{11}B NMR (THF-d_8): δ 7 (br). ^{19}F NMR (THF-d_8): δ −138.8 (br), −132.1 (br). ^{29}Si NMR (THF-d_8): δ −32.8 (ddd, $^{1}J_{Si-F}$ = 276 Hz, $^{1}J_{Si-F}$ = 39 Hz). Anal. Calcd for $C_{45}H_{69}BF_3KO_8Si$ (**17b**·2THF): C, 61.91; H, 7.97. Found: C, 61.80; H, 8.15.

*[2.2.2]Cryptand [o-(Difluorophenylsilyl)phenyl]-fluorodimesitylborate (**18a**).* A solution of **4** (141 mg, 0.30 mmol), [2.2.2]cryptand (116 mg, 0.30 mmol), and KF (18 mg, 0.30 mmol) in toluene (0.9 mL) was stirred at room temperature for 4.5 h. The solvent was removed in vacuo, and the resulting white solid was dissolved in a minimum amount of THF at room temperature. A small amount of hexane was slowly added over the saturated solution, resulting in a two-layer solution. The two-layer solution was allowed to stand at room temperature for 1 d to give **18a** (242 mg, 89%).

mp 179−182 °C (sealed). ^{1}H NMR (THF-d_8): δ 1.78 (s, 12H), 2.05 (s, 6H), 2.51 (t, ^{3}J = 5 Hz, 12H, *cryptand*), 3.49 (t, ^{3}J = 5 Hz, 12H, *cryptand*), 3.53 (s, 12H, *cryptand*), 6.28 (s, 4H), 6.84−6.99 (m, 5H), 7.19 (dd, ^{3}J = 7 Hz, ^{4}J = 2 Hz, 1H), 7.52 (d, ^{3}J = 7 Hz, 2H), 7.88−7.92 (m, 1H). ^{13}C NMR (THF-d_8): δ 21.2 (CH_3), 25.6 (CH_3), 54.7 (*cryptand*, CH_2), 68.4 (*cryptand*, CH_2), 71.3 (*cryptand*, CH_2), 123.3 (CH), 126.6 (CH), 127.9 (CH), 128.8 (CH), 128.9 (CH), 131.4 (C), 133.8 (d, $^{3}J_{F-C}$ = 3 Hz, CH), 135.2 (q, $^{3}J_{F-C}$ = 3 Hz, CH), 135.6 (d, $^{3}J_{F-C}$ = 3 Hz, CH), 135.8 (d, $^{2}J_{F-C}$ = 20 Hz, C),

https://doi.org/10.1021/acsomega.2c02775
ACS Omega 2022, 7, 30939−30953

140.3 (d, $^2J_{F-C}$ = 25 Hz, C), 141.6 (C), 152.8 (br, C), 173.1 (br, C). ^{11}B NMR (THF-d_8): δ 8 (br). ^{19}F NMR (THF-d_8): δ −137.0 to −134.1 (br). ^{29}Si NMR (THF-d_8, −181 K): δ −58.2 (ddd, $^1J_{Si-F}$ = 273 Hz, $^1J_{Si-F}$ = 64 Hz). Anal. Calcd for $C_{48}H_{67}BF_3KN_2O_6Si$ (**18a**): C, 63.84; H, 7.48; N 3.10. Found: C, 63.60; H, 7.54; N, 3.11.

*Potassium 18-Crown-6 [o-(Difluorophenylsilyl)phenyl]-fluorodimesitylborate (**18b**).* This compound was prepared using the same procedure described for **15b** from **4** (188 mg, 0.40 mmol), KF (25 mg, 0.42 mmol), and 18-crown-6 (111 mg, 0.42 mmol) and obtained as colorless crystals of **18b**•THF (299 mg, 0.38 mmol) in 95% yield.

mp 212−216 °C (decomposed/sealed). ^{1}H NMR (THF-d_8): δ 1.77 (s, 12H), 2.05 (s, 6H), 3.52 (s, 24H, *crown*), 6.29 (s, 4H), 6.88−7.01 (m, 5H), 7.19 (dd, ^3J = 6 Hz, ^4J = 2 Hz, 1H), 7.54 (dd, ^3J = 8 Hz, ^4J = 1 Hz, 2H), 7.89−7.92 (m, 1H). ^{13}C NMR (THF-d_8): δ 21.2 (CH_3), 25.6 (CH_3), 71.0 (*crown*, CH_2), 123.4 (CH), 126.6 (CH), 128.0 (CH), 128.8 (CH), 128.9 (CH), 131.6 (C), 133.7 (q, $^3J_{C-F}$ = 3 Hz, CH), 135.2 (q, $^3J_{F-C}$ = 3 Hz, CH), 135.6 (q, $^3J_{F-C}$ = 3 Hz, CH), 135.8 (q, $^2J_{F-C}$ = 20 Hz, C), 140.5 (q, $^2J_{F-C}$ = 25 Hz, C), 141.6 (C), 152.6 (br, C), 172.7 (br, C). ^{11}B NMR (THF-d_8): δ 9 (br). ^{19}F NMR (THF-d_8): δ −134.9 (br). ^{29}Si NMR (THF-d_8, −181 K): δ −58.2 (ddd, $^1J_{Si-F}$ = 273 Hz, $^1J_{Si-F}$ = 65 Hz). Anal. Calcd for $C_{46}H_{63}BF_3KO_7Si$ (**18b**·THF): C, 64.02; H 7.36. Found: C, 64.33; H, 7.43.

*Potassium 18-Crown-6 [o-(Fluorodimethylsilyl)phenyl]-cyanodimesitylborate (**19**).* A solution of **1** (201 mg, 0.50 mmol), 18-crown-6 (87 mg, 0.33 mmol), and KCN (22 mg, 0.32 mmol) in toluene (3.0 mL) was stirred at room temperature for 20 h. The solvent was removed in vacuo, and the resulting white solid was dissolved in THF (ca. 5 mL) at room temperature. The solution was filtered through a membrane filter; the filtrate was partly concentrated and cooled to −31 °C to give **19**·THF as colorless crystals (81 mg, 36%).

mp 195−200 °C (decomposed/sealed). ^{1}H NMR (THF-d_8): δ 0.22−0.33 (br, 6H), 1.89 (br, 12H), 2.11 (s, 6H), 3.59 (s, 24H, *crown*), 6.40−6.49 (br, 4H), 6.77 (t, ^3J = 7 Hz, 1H), 6.87 (t, ^3J = 7 Hz, 1H), 7.07 (d, ^3J = 8 Hz, 1H), 7.62 (d, ^3J = 8 Hz, 1H). ^{13}C NMR (THF-d_8): δ −3.2 (d, $^2J_{F-C}$ = 18 Hz, CH_3), 21.1 (CH_3), 26.4 (CH_3), 71.1 (*crown*, CH_2), 123.0 (CH), 127.8 (CH), 129.4 (CH), 131.7 (C), 134.1 (d, $^3J_{F-C}$ = 7 Hz, CH), 137.0 (CH), 143.5 (C), 144.3 (d, $^3J_{F-C}$ = 11 Hz, C); the peaks corresponding to the *ipso* and *para* carbon atoms in the mesityl groups and the carbon atom in the cyano group were not observed. ^{11}B NMR (THF-d_8): δ −14 (br). ^{19}F NMR (THF-d_8): δ −152.1 (sept, $^3J_{F-H}$ = 9 Hz). ^{29}Si NMR (THF-d_8): δ 20.6 (d, $^1J_{Si-F}$ = 266 Hz). Anal. Calcd for $C_{43}H_{64}BFKNO_7Si$ (**19**·THF): C, 64.24; H, 8.02; N, 1.74. Found: C, 64.17; H, 8.12; N, 1.67.

*Potassium 18-Crown-6 [o-(Difluoromethylsilyl)phenyl]-cyanodimesitylborate (**20**).* This compound was prepared using the same procedure described for **19** from **3** (163 mg, 0.42 mmol), KCN (28 mg, 0.42 mmol), and 18-crown-6 (111 mg, 0.42 mmol) and obtained as colorless crystals of **20**•THF (158 mg, 0.19 mmol) in 49% yield.

mp 232−235 °C (decomposed/sealed). ^{1}H NMR (THF-d_8): δ 0.18 (t, $^3J_{F-H}$ = 7 Hz, 3H), 1.89 (s, 12H), 2.13 (s, 6H), 3.57 (s, 24H, *crown*), 6.48 (s, 4H), 6.92 (d of quint., ^3J = 7 Hz, ^4J = 2 Hz, 2H), 7.15 (d, ^3J = 6 Hz, 1H), 7.67 (d, ^3J = 6 Hz, 1H). ^{13}C NMR (THF-d_8): δ 0.2 (t, $^2J_{F-C}$ = 17 Hz, CH_3), 21.1 (CH_3), 26.4 (CH_3), 71.0 (*crown*, CH_2), 123.3 (CH), 128.8 (CH), 129.5 (CH), 132.2 (C), 134.7 (CH), 137.3 (CH), 137.8 (C), 143.4 (C), 151.6 (br, C), 168.5 (br, C); the peak corresponding to the carbon atom in the cyano group was not observed. ^{11}B NMR (THF-d_8): δ −14 (br). ^{19}F NMR (THF-d_8): δ −129.6 (s). ^{29}Si NMR (THF-d_8): δ −10.5 (t, $^1J_{Si-F}$ = 289 Hz). Anal. Calcd for $C_{38}H_{53}BF_2KNO_6Si$: C, 62.03; H, 7.26; N, 1.90. Found: C, 62.40; H, 7.60; N, 1.66.

Potassium 18-Crown-6 Fluorodimesitylphenylborate (27). A solution of **26** (163 mg, 0.50 mmol), KF (30 mg, 0.51 mmol), and 18-crown-6 (134 mg, 0.51 mmol) in toluene (1.5 mL) was stirred at room temperature for 3.5 h. The solvent was removed in vacuo, and the resulting white solid was dissolved in a minimum amount of THF at room temperature. A small amount of hexane was slowly added over the saturated solution, resulting in a two-layer solution. The two-layer solution was allowed to stand at room temperature for 1 d to give **27**·THF (304 mg, 94% yield) as colorless crystals.

mp 173−174 °C (decomposed). ^{1}H NMR (THF-d_8): δ 1.90 (s, 12H), 2.10 (s, 6H), 3.54 (s, 24H, *crown*), 6.42 (s, 4H), 6.79 (t, 1H, ^3J = 7 Hz), 6.70−7.20 (br, 3H), 7.90 (br, 1H). ^{13}C{^{1}H} NMR (THF-d_8): δ 21.3, 25.8 (d, $^4J_{F-C}$ = 4 Hz), 70.9 (*crown*), 123.2, 126.2, 128.9, 131.1, 134.6, 142.0 (d, $^3J_{C-F}$ = 3 Hz), 156.0 (br), 164.1 (br). ^{11}B{^{1}H} NMR (THF-d_8): δ 5.5. ^{19}F NMR (THF-d_8): δ −173.2. Anal. Calcd for $C_{40}H_{59}O_7BFK$ (**27**·THF): C, 66.65; H, 8.25. Found: C, 66.42; H, 8.52.

*p-Bromo(dimethylsilyl)benzene (**22**).* *n*-BuLi in hexane (1.66 M, 20.0 mL, 33.2 mmol) was added dropwise over 11 min to a solution of *p*-dibromobenzene (7.22 g, 30.0 mmol) in THF (60 mL) and Et_2O (60 mL) at −78 °C. The resulting reaction mixture was stirred at −78 °C for 40 min. A solution of chlorodimethylsilane (4.0 mL, 36.0 mmol) in Et_2O (15 mL) was added dropwise over 13 min to the reaction mixture at −78 °C. The resulting reaction mixture was stirred at −78 °C for 1.5 h and then allowed to warm to room temperature. The solvent was evaporated, and the resulting residue was dissolved in hexane (30 mL). The solution was filtered through a glass fiber pad, and the filtrate was concentrated. The resulting residue was distilled under reduced pressure (43−46 °C/0.4 mmHg) to give **22** as a colorless liquid (4.49 g, 70% yield).

^{1}H NMR ($CDCl_3$): δ 0.33 (d, ^3J = 4 Hz, 6H), 4.39 (sept, ^3J = 4 Hz, 1H), 7.40 (dt, ^3J = 8 Hz, ^4J = 2 Hz, 2H), 7.50 (dt, ^3J = 8 Hz, ^4J = 2 Hz, 2H). ^{13}C NMR ($CDCl_3$): δ −3.9 (CH_3), 123.9 (C), 131.0 (CH), 135.5 (CH), 136.1 (C). ^{29}Si NMR ($CDCl_3$): δ −16.6 (s).

*p-(Dimethylsilyl)(dimesitylboryl)benzene (**24**).* A solution of *tert*-BuLi in pentane (1.59 mol/L, 3.3 mL, 5.25 mmol) was added to a solution of **22** (1.11 g, 5.17 mmol) in Et_2O (9 mL) at −78 °C over 3 min. The resulting reaction mixture was stirred at −78 °C for 2 h, forming a white suspension of **23**. A solution of fluorodimesitylborane (1.41 g, 5.26 mmol) in Et_2O (8 mL) was added to the suspension at −78 °C over 8 min, and the reaction mixture was stirred at −78 °C for 0.5 h and 0 °C for 0.5 h and then allowed to warm to room temperature. The reaction mixture was concentrated in vacuo; the residue was diluted with hexane (20 mL), and the insoluble precipitate was removed via filtration through a glass fiber pad. The filtrate was concentrated in vacuo, and the crude product (2.19 g) was subjected to column chromatography on silica gel eluted with hexane (R_f = 0.43) to give **22** (1.51 g, 76%) as a white solid.

mp 97−99 °C (air). ^{1}H NMR (C_6D_6): δ 0.22 (dd, ^3J = 4 Hz, ^4J = 1 Hz, 6H), 2.15−2.30 (br, 18H), 4.65 (sept, ^3J = 4 Hz, 1H), 6.85 (s, 4H), 7.56 (d, ^3J = 7 Hz, 2H), 7.74 (d, ^3J = 7 Hz,

https://doi.org/10.1021/acsomega.2c02775
ACS Omega 2022, 7, 30939−30953

2H). ^{13}C NMR (C_6D_6): δ −4.0 (CH_3), 21.3 (CH_3), 23.8 (CH_3), 128.8 (CH), 134.1 (CH), 135.8 (CH), 138.9 (C), 141.0 (C), 142.2 (br, C), 142.3 (C), 147.2 (br, C). ^{11}B NMR (C_6D_6): δ 75 (br). ^{29}Si NMR (C_6D_6): δ −16.8 (s). Anal. Calcd for $C_{26}H_{33}BSi$: C, 81.23; H, 8.65. Found: C, 80.84; H, 8.88.

*p-(Fluorodimethylsilyl)(dimesitylboryl)benzene (**21**).* A solution of **24** (1.93 g, 5.02 mmol) in CH_2Cl_2 (15 mL) was added dropwise over 5 min to a solution of Ph_3CBF_4 (1.68 g, 5.09 mmol) in CH_2Cl_2 (13 mL) at 0 °C. The reaction mixture was stirred at 0 °C for 1.5 h and then allowed to warm to room temperature. The reaction mixture was concentrated in vacuo. The residue was diluted with hexane (30 mL), and the insoluble precipitate was removed via filtration through a glass fiber pad. The filtrate was partly concentrated and cooled to −18 °C. The precipitated triphenylmethane (917 mg) was removed via filtration. The filtrate was concentrated, and the residue was subjected to bulb-to-bulb distillation under reduced pressure (190 °C (bath temp.)/0.1 mmHg) to give the remaining triphenylmethane (282 mg). The residue was recrystallized from hexane at −18 °C to give **21** (1.31 g, 65%) as a white solid.

mp 93−97 °C (air). ^{1}H NMR (THF-d_8): δ 0.47 (dd, ^3J = 8 Hz, ^4J = 1 Hz, 6H), 1.98 (s, 12H), 2.28 (s, 6H), 6.81 (s, 4H), 7.49 (d, ^3J = 7 Hz, 2H), 7.60 (d, ^3J = 7 Hz, 2H). ^{13}C NMR (THF-d_8): δ −1.2 (d, $^2J_{F-C}$ = 16 Hz, CH_3), 21.4 (CH_3), 23.8 (CH_3), 129.1 (CH), 133.4 (d, $^3J_{F-C}$ = 2 Hz, CH), 136.1 (CH), 139.6 (C), 141.4 (C), 141.5 (C), 142.5 (br, C), 148.8 (br, C). ^{11}B NMR (THF-d_8): δ 75 (br). ^{19}F NMR (THF-d_8): δ −161.8 (sept, $^3J_{F-H}$ = 7 Hz). ^{29}Si NMR (THF-d_8): δ 20.4 (d, $^1J_{Si-F}$ = 278 Hz). Anal. Calcd for $C_{26}H_{32}BFSi$: C, 77.60; H, 8.01. Found: C, 77.68; H, 8.32.

*Potassium 18-Crown-6 [p-(Fluorodimethylsilyl)phenyl]-fluorodimesitylborate (**25b**).* A solution of **21** (201 mg, 0.50 mmol), KF (31 mg, 0.52 mmol), and 18-crown-6 (138 mg, 0.52 mmol) in toluene (1.5 mL) was stirred at room temperature for 5.5 h. The solvent was removed in vacuo, and the resulting white solid was dissolved in a minimum amount of THF at room temperature. A small amount of hexane was slowly added over the saturated solution, forming a two-layer solution. The two-layer solution was allowed to stand at −31 °C for 1 d to give **25b**·THF (387 mg, 97%) as colorless crystals.

mp 198−201 °C (air). ^{1}H NMR (THF-d_8): δ 0.36 (dd, ^3J = 8 Hz, ^4J = 1 Hz, 6H), 1.91 (s, 12H), 2.10 (s, 6H), 3.53 (s, 24H, *crown*), 6.42 (s, 4H), 7.2 (br, 4H). ^{13}C NMR (THF-d_8): δ −1.0 (d, $^2J_{F-C}$ = 17 Hz, CH_3), 21.2 (CH_3), 25.8 (d, $^4J_{F-C}$ = 4 Hz, CH_3), 71.0 (*crown*, CH_2), 128.7 (d, $^2J_{F-C}$ = 16 Hz, C), 128.9 (CH), 131.1 (br, CH), 131.2 (C), 134.4 (br, CH), 142.0 (d, $^3J_{F-C}$ = 2 Hz, C), 155.8 (br, C), 168.5 (br, C). ^{11}B NMR (THF-d_8): δ 6 (br). ^{19}F NMR (THF-d_8): δ −174.5 (br), −159.0 (sept, $^3J_{F-H}$ = 8 Hz). ^{29}Si NMR (THF-d_8): δ 20.0 (d, $^1J_{Si-F}$ = 277 Hz). Anal. Calcd for $C_{38}H_{56}BF_2KO_6Si$ (**25a**): C, 62.97; H, 7.79. Found: C, 62.74; H, 8.07.

*Potassium [2.2.2]Cryptand [p-(Fluorodimethylsilyl)-phenyl]fluorodimesitylborate (**25a**).* This compound was prepared using the same procedure described for **25b** from **21** (161 mg, 0.40 mmol), KF (25 mg, 0.42 mmol), and [2.2.2]cryptand (158 mg, 0.42 mmol) and obtained as colorless crystals of **25a**•THF (290 mg, 0.35 mmol) in 87% yield.

mp 158−160 °C (air). ^{1}H NMR (THF-d_8): δ 0.36 (dd, ^3J = 7 Hz, ^4J = 1 Hz, 6H), 1.89 (s, 12H), 2.09 (s, 6H), 2.51 (t, ^3J = 5 Hz, 12H, *cryptand*), 3.50 (t, ^3J = 5 Hz, 12H, *cryptand*), 3.52 (s, 12H, *cryptand*), 6.37 (s, 4H), 6.96−7.35 (br, 3H), 7.90 (br, 1H). ^{13}C NMR (THF-d_8): δ −0.9 (d, $^2J_{F-C}$ = 17 Hz, CH_3), 21.3 (CH_3), 25.8 (d, $^4J_{F-C}$ = 5 Hz, CH_3), 54.7 (*cryptand*, CH_2), 68.4 (*cryptand*, CH_2), 71.3 (*cryptand*, CH_2), 128.2 (d, $^2J_{F-C}$ = 16 Hz, C), 128.7 (CH), 130.7 (C), 131.0 (CH), 134.7 (br, CH), 142.3 (d, $^3J_{F-C}$ = 2 Hz, C), 156.6 (br, C), 169.8 (br, C). ^{11}B NMR (THF-d_8): δ 5 (br). ^{19}F NMR (THF-d_8): δ −176.6 (br), −158.6 (sept, $^3J_{F-H}$ = 7 Hz). ^{29}Si NMR (THF-d_8): δ 20.1 (d, $^1J_{Si-F}$ = 277 Hz). Anal. Calcd for $C_{48}H_{76}BF_2KN_2O_7Si$ (**25b**·THF): C, 63.41; H, 8.43; N, 3.08. Found: C, 63.01; H, 8.50; N, 3.31.

Competition Experiments. *Reaction of **1** and **27** in THF (Scheme 7).* A solution of **1** (20 mg, 0.050 mmol) and **27** (33 mg, 0.050 mmol) in THF (1.0 mL) in a Schlenk flask was stirred at room temperature for 24 h. The reaction mixture was transferred into a J. Young NMR tube, and its ^{19}F NMR spectrum was recorded at 298 K in an unlocked mode. The molar ratio (95:5) was determined using the ratio of the integrals for **15b** and **27**: K_{298} = [**15b**][**26**]/[**1**][**27**] = [95][95]/[5][5] = 3.6 × 10^2.

*Reaction of **1** and **16b** in THF (Scheme 8).* A solution of **1** (20 mg, 0.050 mmol) and **16b** (46 mg, 0.050 mmol) in THF (1.0 mL) in a Schlenk flask was stirred at room temperature for 24 h. The reaction mixture was transferred into a J. Young NMR tube, and its ^{19}F NMR spectrum was recorded at 298 K in an unlocked mode. The molar ratio (95:5) was determined using the ratio of the integrals for **15b** and **16b**: K_{298} = [**15b**][**2**]/[**1**][**16b**] = [82][82]/[18][18] = 21.

*Reaction of **3** and **15b** in THF (Scheme 9).* A solution of **3** (20 mg, 0.050 mmol) and **15b** (40 mg, 0.050 mmol) in THF (1.0 mL) in a Schlenk flask was stirred at room temperature for 24 h and then heated at reflux for 24 h to complete the equilibrium. The reaction mixture was transferred into a J. Young NMR tube, and its ^{19}F NMR spectrum was recorded at 298 K in an unlocked mode. The molar ratio (79:21) was determined using the ratio of the integrals for **15b** and **17b**: K_{298} = [**17b**][**1**]/[**3**][**15b**] = [79][79]/[21][21] = 14.

*Reaction of **3** and **18b** in THF (Scheme 10).* A solution of **3** (20 mg, 0.050 mmol) and **18b** (40 mg, 0.050 mmol) in THF (1.0 mL) in a Schlenk flask was stirred at room temperature for 24 h. The reaction mixture was transferred into a J. Young NMR tube, and its ^{19}F NMR spectrum was recorded at 298 K in an unlocked mode. The molar ratio (45:55) was determined using the ratio of the integrals for **3** and **4**: K_{298} = [**17b**][**4**]/[**3**][**18b**] = [55][55]/[45][45] = 1.5.

Dynamic Behavior at Variable Temperatures. *Typical Procedure.* A solution of **15a** (20 mg, 0.024 mmol) in THF-d_8 (0.60 mL) was injected into a J. Young NMR tube, and its ^{19}F NMR spectrum was recorded at variable temperatures.

■ ASSOCIATED CONTENT

Supporting Information

The Supporting Information is available free of charge at https://pubs.acs.org/doi/10.1021/acsomega.2c02775.

Summary of the structural data, table of crystallographic data, and computational works (PDF)

■ AUTHOR INFORMATION

Corresponding Author

Atsushi Kawachi − *Department of Chemistry, Graduate School of Science, Hiroshima University, Hiroshima 739-8526, Japan; Faculty of Bioscience and Applied Chemistry,*

https://doi.org/10.1021/acsomega.2c02775
ACS Omega 2022, 7, 30939−30953

Hosei University, Tokyo 184-8584, Japan; orcid.org/0000-0001-7306-7669; Email: kawachi@hosei.ac.jp

Authors

Junpei Shimada − *Department of Chemistry, Graduate School of Science, Hiroshima University, Hiroshima 739-8526, Japan*

Atsushi Tani − *Department of Chemistry, Graduate School of Science, Hiroshima University, Hiroshima 739-8526, Japan*

Chihiro Hanazato − *Faculty of Bioscience and Applied Chemistry, Hosei University, Tokyo 184-8584, Japan*

Takashi Masuyama − *Faculty of Bioscience and Applied Chemistry, Hosei University, Tokyo 184-8584, Japan*

Yohsuke Yamamoto − *Department of Chemistry, Graduate School of Science, Hiroshima University, Hiroshima 739-8526, Japan*

Complete contact information is available at: https://pubs.acs.org/10.1021/acsomega.2c02775

Notes

The authors declare no competing financial interest.

■ ACKNOWLEDGMENTS

This work was partially supported by a Grant-in-Aid for Scientific Research on Innovative Areas "Molecular Activation Directed toward Straightforward Synthesis" (no. 25105740) and "Stimuli-responsive Chemical Species for the Creation of Functional Molecules" (no. 15H00961) from the Ministry of Education, Culture, Sports, Science and Technology, Japan.

■ REFERENCES

(1) Reviews on polydentate Lewis acids: (a) Schmidtchen, F. P.; Berger, M. Artificial Organic Host Molecules for Anions. *Chem. Rev.* **1997**, *97*, 1609. (b) Hawthorne, M. F.; Zheng, Z. Recognition of Electron-Donating Guests by Carborane-Supported Multidentate Macrocyclic Lewis Acid Hosts: Mercuracarborand Chemistry. *Acc. Chem. Res.* **1997**, *30*, 267. (c) Wuest, J. D. Multiple Coordination and Activation of Lewis Bases by Multidentate Lewis Acids. *Acc. Chem. Res.* **1999**, *32*, 81. (d) Piers, W. E.; Irvine, G. J.; Williams, V. C. Highly Lewis Acidic Bifunctional Organoboranes. *Eur. J. Inorg. Chem.* **2000**, 2131. (e) Gabbaï, F. P. The Charge-Reverse Analogy as an Inspiration for the Preparation of Polydentate Lewis Acidic Boranes. *Angew. Chem., Int. Ed.* **2003**, *42*, 2218.

(2) Lewis acidity of organoboron compounds: (a) Hudnall, T. D.; Chiu, C.-W.; Gabbaï, F. P. Fluoride Ion Recognition by Chelating and Cationic Boranes. *Acc. Chem. Res.* **2009**, *42*, 388. (b) Wade, C. R.; Broomsgrove, A. R. J.; Aldridge, S.; Gabbaï, F. P. Fluoride Ion Complexation and Sensing Using Organoboron Compounds. *Chem. Rev.* **2010**, *110*, 3958.

(3) Lewis acidity of organosilicon compounds: (a) Damrauer, R.; Danahey, S. E. Preparation and NMR Studies of Pentacoordinated Silicon Anions. *Organometallics* **1986**, *5*, 1490. (b) Harland, J. J.; Payne, J. S.; Day, R. O.; Holmes, R. R. Pentacoordinated Molecules. 70. Steric Hindrance in Pentacoordinated Fluorosilicates. Synthesis and Molecular Structure of the Diphenyl-1-naphthyldifluorosilicate Anion and the Phenylmethyltrifluorosilicate Anion. *Inorg. Chem.* **1987**, *26*, 760. (c) Johnson, S. E.; Day, R. O.; Holmes, R. R. Pentacoordinated Molecules. 77. Intramolecular Ligand Exchange of Pentacoordinated Anionic Silicates, $RSiF_4^-$, via Silicon-29 and Fluorine-19 NMR Spectroscopy. Solution- and Solid-state Structures. *Inorg. Chem.* **1989**, *28*, 3182. (d) Johnson, S. E.; Payne, J. S.; Day, R. O.; Holmes, J. M.; Holmes, R. R. Pentacoordinated Molecules. 78. Intramolecular Ligand Exchange of Pentacoordinated Anionic Silicates, $R_2SiF_3^-$, via Silicon-29 and Fluorine-19 NMR Spectroscopy. Solution- and Solid-state Structures. *Inorg. Chem.* **1989**, *28*, 3190.

(4) Examples of B/B bidentate Lewis acids: (a) Shriver, D. F.; Biallas, M. J. Observation of the Chelate Effect with a Bidentate Lewis Acid, $F_2BCH_2CH_2BF_2$. *J. Am. Chem. Soc.* **1967**, *89*, 1078. (b) Katz, H. Hydride Sponge: Complexation of 1,8-Naphthalenediylbis(dimethylborane) with Hydride, Fluoride, and Hydroxide. E. *J. Org. Chem.* **1985**, *50*, 5027. (c) Katz, H. E. 1,8-Naphthalenediylbis(dichloroborane) Chloride: The First Bis Boron Chloride Chelate. *Organometallics* **1987**, *6*, 1134. (d) Henderson, L. D.; Piers, W. E.; Irvine, G. J.; McDonald, R. Anion Stability in Stannylium, Oxonium, and Silylium Salts of the Weakly Coordinating Anion $[C_6F_4\text{-}1,2\text{-}\{B(C_6F_5)_2\}_2(\mu\text{-}OCH_3)]^-$. *Organometallics* **2002**, *21*, 340. (e) Hoefelmeyer, J. D.; Gabbaï, F. P. Synthesis of 1,8-Diborylnaphthalenes by the Ring-Opening Reaction of a New Anionic Boron-Bridged Naphthalene Derivative. *Organometallics* **2002**, *21*, 982. (f) Solé, S.; Gabbaï, F. P. A Bidentate Borane as Colorimetric Fluoride Ion Sensor. *Chem. Commun.* **2004**, 1284. (g) Chase, P. A.; Henderson, L. D.; Piers, W. E.; Parvez, M.; Clegg, W.; Elsegood, M. R. J. Bifunctional Perfluoroaryl Boranes: Synthesis and Coordination Chemistry with Neutral Lewis Base Donors. *Organometallics* **2006**, *25*, 349. (h) Melaïmi, M.; Solé, S.; Chiu, C.-W.; Wang, H.; Gabbaï, F. P. Structural and Electrochemical Investigations of the High Fluoride Affinity of Sterically Hindered 1,8-Bis(boryl)naphthalenes. *Inorg. Chem.* **2006**, *45*, 8136.

(5) Examples of Si/Si bidentate Lewis acids: (a) Tamao, K.; Hayashi, T.; Ito, Y.; Shiro, M. Novel Pentacoordinate Anionic Silicate, $[o\text{-}C_6H_4(SiPhF_2)_2F]^-K^+\bullet$18-crown-6, Containing a Bent Fluoride Bridge between Two Silicon Atoms. *J. Am. Chem. Soc.* **1990**, *112*, 2422. (b) Tamao, K.; Hayashi, T.; Ito, Y.; Shiro, M. Pentacoordinate Anionic Bis(siliconates) Containing a Fluorine Bridge between Two Silicon Atoms. Synthesis, Solid-state Structures, and Dynamic Behavior in Solution. *Organometallics* **1992**, *11*, 2099. (c) Ebata, K.; Inada, T.; Kabuto, C.; Sakurai, H. Hexakis(fluorodimethylsilyl)benzene, Hexakis(methoxydimethylsilyl)benzene, and Related Compounds. Novel Neutral Pentacoordinate Structures for Silicon and Merry-Go-Round Degenerate Fluorine Migration. *J. Am. Chem. Soc.* **1994**, *116*, 3595. (d) Tamao, K.; Hayashi, T.; Ito, Y. Anion Complex by Bidentate Lewis Acidic Hosts, *ortho*-Bis(fluorosilyl)benzenes. *J. Organomet. Chem.* **1996**, *506*, 85. (e) Brondani, D.; Carré, F. H.; Corriu, R. J. P.; Moreau, J. J. E.; Man, M. Synthesis and Dynamic Behavior of the Heptafluorotrisilacyclohexane Anion: A New Fluxional Silicate with Rapid Intramolecular Exchange of Fluoride Ligand. *Angew. Chem., Int. Ed.* **1996**, *35*, 324. (f) Horstmann, J.; Niemann, M.; Berthold, K.-N.; Mix, A.; Neumann, B.; Stammler, H.-G.; Mitzel, N. W. Fluoride Complexation by Bidentate Silicon Lewis Acids. *Dalton Trans.* **2017**, *46*, 1898. (g) Asao, N.; Shibato, A.; Itagaki, Y.; Jourdan, J.; Maruoka, F.; Maruoka, K. *o*-Bis(allyldimethylsilyl)benzene as a Remarkably Effective Allylation Agent for Carbonyl Compounds with Bu_4NF Catalyst. *Tetrahedron Lett.* **1998**, *39*, 3177. (h) Kira, M.; Kwon, E.; Kabuto, C.; Sakamoto, K. X-Ray Crystal Structure and Dynamic Behavior of Pentafluoro-9,10-disila-9,10-dihydroanthracene Anion Salts Having Transannular 1,4-Fluorine Bridge. *Chem. Lett.* **1999**, *28*, 1183. (i) Panisch, R.; Bolte, M.; Müller, T. Hydrogen- and Fluorine-Bridged Disilyl Cations and Their Use in Catalytic C−F Activation. *J. Am. Chem. Soc.* **2006**, *128*, 9676. (j) Khalimon, A. Y.; Lin, Z. H.; Simionescu, R.; Vyboishchikov, S. F.; Nikonov, G. I. Persistent Silylium Ions Stabilized by Polyagostic Si−H···Si Interactions. *Angew. Chem., Int. Ed.* **2007**, *46*, 4530.

(6) Examples of B/Si bidentate Lewis acids: (a) Katz, H. E. Anion Complexation and Migration in (8-Silyl-1-naphthyl)boranes. Participation of Hypervalent Silicon. *J. Am. Chem. Soc.* **1986**, *108*, 7640. (b) Wrackmeyer, B.; Milius, W.; Tok, O. L. Reaction of Alkyn-1-yl(diorganyl)silanes with 1-Boraadamantane: Si-H-B Bridges Confirmed by the Molecular Structure in the Solid State and in Solution. *Chem. Eur. J.* **2003**, *9*, 4732. (c) Kelly, M. J.; Broomsgrove, A. E. J.; Morgan, I. R.; Siewert, I.; Fitzpatrick, P.; Smart, J.; Vidovic, D.; Aldridge, S. Syntheses and Anion Binding Capabilities of Bis(diarylboryl) Ferrocenes and Related Systems. *Organometallics* **2013**, *32*, 2674.

(7) B/Hg: (a) Lee, M. H.; Gabbaï, F. P. Syntheses and Anion Binding Capabilities of Bis(diarylboryl) Ferrocenes and Related Systems. *Inorg. Chem.* **2007**, *46*, 8132 B/C:. (b) Chiu, C.-W.; Gabbaï, F. P. Fluoride Ion Capture from Water with a Cationic Borane. *J. Am. Chem. Soc.* **2006**, *128*, 14248 B/N:. (c) Hudnall, T. W.; Melaïmi, M.; Gabbaï, F. P. Hybrid Lewis Acid/Hydrogen-Bond Donor Receptor for Fluoride. *Org. Lett.* **2006**, *8*, 2747 B/P:. (d) Melaimi, M.; Gabbaï, F. P. A Heteronuclear Bidentate Lewis Acid as a Phosphorescent Fluoride Sensor. *J. Am. Chem. Soc.* **2005**, *127*, 9680 B/Sn:. (e) Boshra, R.; Sundararaman, A.; Zakharov, L. N.; Incarvito, C. D.; Rheingold, A. L.; Jäkle, F. Binding Cooperativity of Two Different Lewis Acid Groups at the Edge of Ferrocene. *Chem. Eur. J.* **2005**, *11*, 2810 B/Sn:. (f) Boshra, R.; Venkatasubbaiah, K.; Doshi, A.; Lalancette, R. A.; Kakalis, L.; Jäkle, F. Simultaneous Fluoride Binding to Ferrocene-Based Heteronuclear Bidentate Lewis Acids. *Inorg. Chem.* **2007**, *46*, 10174.

(8) Sn/Sn: Altmann, R.; Jurkschat, K.; Schümann, M. *Organometallics* **1998**, *17*, 5858.

(9) Kawachi, A.; Tani, A.; Shimada, J.; Yamamoto, Y. Synthesis of B/Si Bidentate Lewis Acids, *o*-(Fluorosilyl)(dimesitylboryl)benzenes, and Their Fluoride Ion Affinity. *J. Am. Chem. Soc.* **2008**, *130*, 4222.

(10) (a) Kawachi, A.; Tani, A.; Machida, K.; Yamamoto, Y. *o*-(Fluorodimethylsilyl)phenyllithium as a Versatile Reagent for Preparation of Unsymmetrical, Silicon-Functionalized *o*-Disilylbenzenes. *Organometallics* **2007**, *26*, 4697. (b) Kawachi, A.; Teranishi, A.; Yamamoto, Y. *Tetrahedron Lett.* **2009**, *50*, 1226. (c) Kawachi, A.; Teranishi, T.; Deguchi, T.; Yamamoto, Y. *Heteroat. Chem.* **2013**, *24*, 53.

(11) Kawachi, A.; Morisaki, H.; Zaima, M.; Teranishi, T. Y.; Yamamoto, Y. Synthesis and Structures of o-(Dihydrosilyl)-(dimesitylboryl)benzenes. *J. Organnomet. Chem.* **2010**, *695*, 2167.

(12) Tamao, K.; Sun, G.-R.; Kawachi, A.; Yamaguchi, S. Regioselective Synthesis of Polyfunctionalized Alkyltrisilanes and -tetrasilanes via Reductive Cross-Coupling Reaction of Aminoalkylsilyl Chlorides with Lithium. *Organometallics* **1997**, *16*, 780.

(13) CCDC no. 1971599 (**17a**), 1971600 (**17b**), 1971601 (**18a**), and 1971602 (**18b**). Also see Supporting Information for a summary of the X-ray crystallographic analysis.

(14) For examples of di- and trifluorosilicates with K^+/[2.2.2] cryptand or K^+/18-crown-6: Yamaguchi, S.; Akiyama, S.; Tamao, K. Effect of Countercation Inclusion by [2.2.2]Cryptand upon Stabilization of Potassium Organofluorosilicates. *Organometallics* **1999**, *18*, 2851 Also see 3.

(15) Minimal non-bonded approach: Glidewell, C. Some Chemical and Structural Consequences of Non-bonded Interactions. *Inorg. Chim. Acta* **1975**, *12*, 219.

(16) Also see Supporting Information for NMR spectra.

(17) Typical range of ^{11}B NMR shifts: Elschenbroich, C.; Salzer, A. Organometallics. *A Concise Introduction*; VCH: Weinheim, 1992; pp 73−75, Chapter 7.

(18) Typical range of ^{29}Si NMR shifts: Williams, E. A. *The chemistry of organic silicon compounds*; Patai, S., Rappoport, Z., Eds.; Wiley: Chichester, U.K.., 1989; Part 1, Chapter 8.

(19) Recent examples of complexation with a cyanide ion: (a) Broomsgrove, A. E. J.; Addy, D.; Di Paolo, A.; Morgan, I. R.; Bresner, C.; Chislett, V.; Fallis, I. A.; Thompson, A. L.; Vidovic, D.; Aldridge, S. Evaluation of Electronics, Electrostatics and Hydrogen Bond Cooperativity in the Binding of Cyanide and Fluoride by Lewis Acidic Ferrocenylboranes. *Inorg. Chem.* **2010**, *49*, 157. (b) Wade, C. R.; Gabbaï, F. P. Cyanide Anion Binding by a Triarylborane at the Outer Rim of a Cyclometalated Ruthenium(II) Cationic Complex. *Inorg. Chem.* **2010**, *49*, 714. (c) Matsumoto, T.; Wade, C. R.; Gabbaï, F. P. Synthesis and Lewis Acidic Behavior of a Cationic 9-Thia-10-boraanthracene. *Organometallics* **2010**, *29*, 5490. (d) Kim, Y.; Huh, H.-S.; Lee, M. H.; Lenov, I. L.; Zhao, H.; Gabbaï, F. P. Turn-On Fluorescence Sensing of Cyanide Ions in Aqueous Solution at Parts-per-Billion Concentrations. *Chem. Eur. J.* **2011**, *17*, 2057. (e) Siewert, I.; Fitzpatrick, P.; Broomsgrove, A. E. J.; Kelly, M.; Vidovic, D.; Aldridge, S. Probing the Influence of Steric Bulk on Anion Binding by Triarylboranes: Comparative Studies of FcB(*o*-Tol)$_2$, FcB(*o*-Xyl)$_2$ and FcBMes$_2$. *Dalton Trans.* **2011**, *40*, 10345. (f) Zhao, H.; Reibenspies, J. H.; Gabbaï, F. P. Lewis Acidic Behavior of B(C_6Cl_5)$_3$. *Dalton Trans.* **2013**, *42*, 608.

(20) CCDC no. 1971592 (**19**). Also see Supporting Information for a summary of the X-ray crystallographic analysis.

(21) Romanato, P.; Duttwyler, S.; Linden, A.; Baldridge, K. K.; Siegel, J. S. Competition between π-Arene and Lone-Pair Halogen Coordination of Silylium Ions? *J. Am. Chem. Soc.* **2011**, *133*, 11844.

(22) CCDC no. 1971593 (**25b**). Also see Supporting Information for a summary of the X-ray crystallographic analysis.

(23) See Supporting Information for details on the competition experiments.

(24) It is plausible that the reactions achieved equilibria under the present reaction conditions by heating or extending the reaction time.

(25) Theoretical calculations: Frisch, J. *Gaussian 09*, rev. B.01; Gaussian Inc.: Wallingford, CT, 2010, and Gaussian 16, rev. C.01; Gaussian Inc.: Wallingford, CT, 2019.

(26) GIAO (Gauge-Independent Atomic Orbital) nuclear magnetic shielding tensors were calculated at the RHF/6-311+G(2d,p) level of theory using the calculated structures. The obtained tensors were converted into their corresponding chemical shifts referenced to the tensors of $BF_3{\cdot}OEt_2$ ($\delta(^{11}B) = 0$), $CFCl_3$ ($\delta(^{19}F) = 0$), and $SiMe_4$ ($\delta(^{29}Si) = 0$) calculated at the same level of theory. See Supporting Information for the details.

(27) NBO analysis: Natural atomic orbital and natural bond orbital analysis, Gaussian NBO ver.3.1 and second order perturbation theory analysis of fock matrix in NBO basis.

(28) The calculation including the cation parts is ideal but seems not realistic when considering the computational time and the slow convergence of the fluxional alkyl chains of the crown ether and the cryptand. (a) Leopold, K. R.; Canagaratna, M.; Phillips, J. A. Partially Bonded Molecules from the Solid State to the Stratosphere. *Acc. Chem. Res.* **1997**, *30*, 57. (b) Mitzel, N. W.; Rankin, D. W. H. Saracen − Molecular Structures from Theory and Experiment: the Best of Both Worlds. *Dalton Trans.* **2003**, 3650.

(29) (a) Christe, K. O.; Dixon, D. A.; McLemore, D.; Wilson, W. W.; Sheehy, J. A.; Boatz, J. A. On a quantitative scale for Lewis acidity and recent progress in polynitrogen chemistry. *J. Fluorine Chem.* **2000**, *101*, 151. (b) Erdmann, P.; Leitner, J.; Schwarz, J.; Greb, L. An Extensive Set of Accurate Fluoride Ion Affinities for p̂Block Element Lewis Acids and Basic Design Principles for Strong Fluoride Ion Acceptors. *ChemPhysChem* **2020**, *21*, 987.

(30) Pelter, A.; Smith, K.; Brown, H. C. *Borane Reagents*; Academic, 1988.

(31) Brown, N. M. D.; Davidson, F.; Wilson, J. W. Dimesitylboryl compounds. *J. Organomet. Chem.* **1981**, *209*, 1.

https://doi.org/10.1021/acsomega.2c02775
ACS Omega 2022, 7, 30939−30953